



# Assessing stream-groundwater connectivity along Mulloon Creek, NSW

**Julian de Lorenzo**  
School of Science  
RMIT University

Submitted in partial fulfilment of the requirements of BIOL2328 Research Project B

October 2021

This Thesis is submitted in accordance with the regulations of RMIT University in partial fulfilment of the requirements of BIOL2328 Research Project B within the degree of Masters of Environmental Science and Technology (MC191).

**Declaration and statement of authorship**

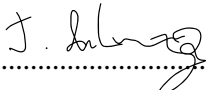
1. I have not impersonated, or allowed myself to be impersonated by any person for the purposes of this assessment.
2. This assessment is my/our original work and no part of it has been copied from any other source except where due acknowledgement is made.
3. No part of this assessment has been written for me by any other person, except where such collaboration has been authorized by the course coordinator.
4. I have not previously submitted this work for this or any other course.
5. I give permission for my assessment response to be reproduced, communicated compared and archived for the purposes of detecting plagiarism.
6. I give permission for a copy of my assessment to be retained by the university for review and comparison, including review by external examiners.

I understand that:

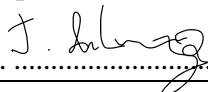
Plagiarism is the presentation of the work, idea or creation of another person as though it is your own. It is a form of cheating and is a very serious academic offence that may lead to exclusion from the University. Plagiarised material can be drawn from, and presented in, written, graphic and visual form, including electronic data and oral presentations. Plagiarism occurs when the origin of the material used is not appropriately cited.

Plagiarism includes the act of assisting or allowing another person to plagiarise or to copy my work. I agree and acknowledge that:

1. I have read and understood the Declaration and Statement of Authorship above.
2. I accept that use of my RMIT account to electronically submit this assessment constitutes my agreement to the Declaration and Statement of Authorship
3. If I do not agree to the Declaration and Statement of Authorship in this context, the assessment outcome is not valid for assessment purposes and cannot be included in my aggregate score for this course.

Signature of candidate:..........Date: 29/10/21

This Project DID NOT involve the use of invertebrates, vertebrates or human subjects. I, Julian de Lorenzo, hereby certify that the Project did not require RMIT University ethics committee clearance, nor a permit from any external organisation.

Signature of candidate:..........Date: 29/10/21

## Abstract

**Background:** Prior to European arrival in Australia, many upland river systems developed into discontinuous chains-of-ponds (COPs). COPs reduce the erosional potential of flood, promote nutrient cycling and help maintain a connection between surface waters and aquifers. Poor land management has led to the deterioration of most COP systems, which has exacerbated droughts, floods and bushfires. Natural Sequence Farming (NSF) is a landscape management methodology that aims to rehydrate and restore degraded land. More quantitative data is required to support NSF techniques.

**Aims:** This aim of this study was to assess the impact of leaky weirs on the connectivity of stream water and proximate aquifers by building a model of water movement in a section of floodplain along the Mulloon Creek.

**Methods:** Surface and groundwaters were studied along two subparallel transects (T3 and T4) of piezometers that cut across Mulloon Creek. The study site is an incised alluvial floodplain, with underlying Ordovician metasediments to the west and Siluro-Devonian leucogranite on the east. Physicochemical and hydrometric measurements were taken in situ. Samples were collected for lab analysis of stable water isotopes ( $\delta^{18}\text{O}$  and  $\delta^2\text{H}$ ) and dissolved ions and trace elements.

**Results:** Hydraulic gradients between groundwater sites, and between stream and groundwater sites, along both transects were low (T3: 0 – 0.06, T4: 0 – 0.04), indicating minimal hydraulic flux between surface and groundwater. Electrical conductivity (EC) of groundwater most closely matched surface water EC at piezometer sites closest to the creek. Groundwater EC increased as sample sites increased in distance from the creek. Deuterium excess in groundwater was 11.6 – 17.28; stream: 15.56 – 17.36. Western alluvial sites had the most chemical similarity to the stream samples, being mixed  $\text{HCO}_3$  and Cl type.

**Conclusions:** Leaky weirs along Mulloon Creek may increase mixing between stream and shallow groundwaters. Lack of significant hydraulic gradients across the floodplain preclude significant recharging of floodplain aquifers. Sodid soils may lead to dispersion and erosion at the site of weirs if there is inadequate vegetation. A repeated sampling schedule and analysis of water stable isotopes would provide more conclusive insights into the origin of groundwater.

## Acknowledgements

This project saw many unforeseen setbacks, mostly due to COVID-19. I am in debt to the many people who helped me get to the finish line. Thank you to Leah Moore and Sharon Gray for conducting fieldwork and lab work and assisting me with data analysis. Sharon also gave me access to her work on local meteoric water lines, which aided in my analysis of water stable isotopes. Thanks to Luke Peel and The Mulloon Institute for bringing me on as a research partner. To Tony Bernadi, for assistance with fieldwork and historical site information. And finally, thank you to Graeme Allinson for support and advice throughout the design, implementation, and submission of the project.

## Table of Contents

<b>Abstract</b> .....	<b>iii</b>
<b>Acknowledgements</b> .....	<b>iv</b>
<b>1. Introduction</b> .....	<b>1</b>
1.1 Background .....	1
1.2 Scope.....	3
1.3 Aims and objectives.....	3
<b>2. Literature Review</b> .....	<b>4</b>
2.1 Fluvial processes.....	4
2.2 River types .....	5
2.3 Australian fluvial systems .....	6
2.4 Groundwater: composition, movement and measurement.....	9
2.4.1 Water stable isotope analysis.....	12
2.4.2 Geochemical processes .....	14
2.5 Natural Sequence Farming.....	17
<b>3. Study Area</b> .....	<b>20</b>
<b>4. Methods</b> .....	<b>25</b>
4.1 Fieldwork .....	25
4.2 Hydraulic potential .....	27
4.3 Laboratory analysis.....	28
<b>5. Results &amp; Discussion</b> .....	<b>29</b>
5.1 Hydraulic potential and electrical conductivity .....	29
5.2 Stable isotopes .....	31
5.3 Geochemistry .....	33
<b>6. Conclusions</b> .....	<b>42</b>
<b>7. References</b> .....	<b>43</b>
<b>Appendix 1: Physical parameters (field measurements)</b> .....	<b>49</b>
<b>Appendix 2: Major ions</b> .....	<b>50</b>
<b>Appendix 3: Hydraulic gradient calculations</b> .....	<b>51</b>
<b>Appendix 4: Trace elements</b> .....	<b>52</b>
<b>Appendix 5: Stable water isotopes</b> .....	<b>54</b>

# 1. Introduction

## 1.1 Background

Landscape function across Australia has deteriorated significantly since the arrival of Europeans (Brierley et al. 1999). In particular, the “chain-of-ponds” systems that characterised many upland Australian waterways no longer exist (Dobes et al. 2013). In many places, poor land management has caused stream incision and gully erosion (Dobes et al. 2013). These processes can lower the water table, disconnecting it from the soil bank (Dobes et al. 2013; Streeton et al. 2013). Further, 89% of wetlands that existed in south-eastern Australia before 1788 may have been destroyed (Environment Australia 1997). Disruption of the hydrological cycle increases severity of droughts and fires (Andrews 2006; Hazell et al. 2003; Nolan et al. 2016). In turn, droughts then further degrade hydrology, leading to a positive feedback loop of worsening environmental conditions (Somerville et al. 2006). Most recently these impacts were experienced during the 2019-20 bushfire season, when more than 18 million ha burned (Filkov et al. 2020). These fires were so extreme in part because 2019 was the driest year on record for the continent, with a mean 277.6 mm rainfall (Filkov et al. 2020). Rainfall in Australia is known to be intermittent, meaning landscapes require significant in-ground water storage to maintain proper ecosystem function in dry times (Dobes et al. 2013). If there is sufficient available groundwater, then in times of low rainfall, surface water baseflow and plant growth can be maintained by water from aquifers (Dobes et al. 2013; Fitts 2013). This groundwater buffer, when functional, can increase the resilience of ecosystems and agricultural production (Dobes et al. 2013; Fitts 2013; Streeton et al. 2013).

Given the importance of landscape hydrology in Australia, any land management practices that encourage the retention and accumulation of water in soil and shallow aquifers should be studied and, if effective, implemented. There are many frameworks, methodologies and philosophies regarding sustainable water and land management (Massy 2017). But it may be difficult for farmers or landowners to judge the appropriateness of a given methodology for their specific context. The present study will assess the impact one landscape methodology, Natural Sequence Farming (NSF).

Natural Sequence Farming is a holistic landscape management framework developed during the latter half of the twentieth century, mainly on a property in the Bylong Valley, NSW (Andrews 2006). NSF attempts to reinstate natural self-regulating processes of hydrology and nutrient exchange that have been disrupted by humans. NSF is based on the assumption that human interference in landscape processes has led to land degradation, habitat loss, climate change and aridification (Andrews 2006; Norris & Andrews 2010). The primary aim of the practice is to re-couple the carbon cycle with the hydrological cycle,

under the assumption that this will reverse degradation and moderate local climate (Norris & Andrews 2010). The four main principles of NSF are to:

1. increase fertility of soils through efficient breakdown of organic matter,
2. improve hydrological function by re-instating a link between surface and groundwater, thereby reducing salinity,
3. promote natural ecological succession by allowing all plants to grow – particularly pioneer species, including non-natives, and
4. discover and understand the natural landscape processes that are necessary for functional ecosystems and agriculture (Williams 2010).

NSF methodology utilises leaky weirs, normally constructed of logs, boulders and soil. The weirs are intended to reduce streamflow velocity, increase stream depth and re-hydrate floodplain aquifers (Dobes et al. 2013). Anecdotal evidence points to the efficacy of the stream interventions and other NSF practices. However, while NSF may be effective at retaining water in landscapes, the landscape interventions may not always be appropriate. Only minimal research has been conducted to quantify the impact of leaky weirs on groundwater recharge (Hickson 2017; Keene et al. 2007; Weber & Field 2010). Keene et al. (2007) analysed a tributary of the Goulburn River in NSW. The study measured electrical conductivity (EC) and ionic concentration along transects parallel and perpendicular to the location of a leaky weir. Hydraulic potential of groundwater decreased, and EC results increased as distance from the stream became greater (Figure 1). These data imply that the leaky weirs may have local impacts on stream-groundwater exchange.

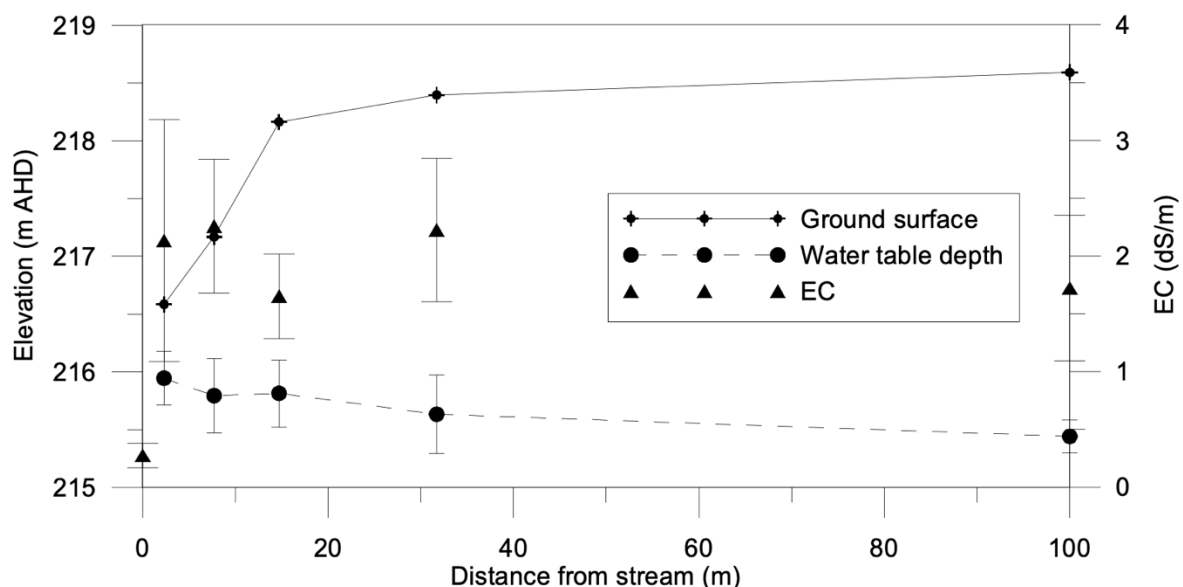


Figure 1: Ground surface elevation, water table depth and EC values along a transect from a stream at Widden Brook, NSW (Keene et al. 2007).

Hickson (2017) studied the relationship between surface and groundwaters at two locations along Mulloon Creek, NSW: one that had been altered by leaky weirs and NSF management, and one that had not. This study showed leaky weirs can increase connectivity between

surface waters and alluvial aquifers. However, transmissivity of local sedimentology was shown to have a large impact on the degree of floodplain rehydration.

It is important to track the interaction between aquifer and stream water using a variety of metrics, in order to build a more accurate model. Prior research on ground-surface water interaction at Mulloon has relied on measuring EC and studying hydraulic gradients (Hickson 2017). This project will collect the same type of data, while also measuring major cations, anions and trace elements present in stream and groundwater. Analysis of stable isotopes  $\delta^{18}\text{O}$  and  $\delta^2\text{H}$  in water will also be undertaken. These data will be used to construct a preliminary conceptual model of water and salt transit through the local landscape.

The successful restoration of Australia's river systems would improve biodiversity and the economic resilience of the country's farmers. A functioning hydrological system has the potential to reverse desertification and buffer climate extremes. As such, the proposed research will add to historical datasets of Mulloon Creek floodplain measurement. As this dataset grows, more accurate conclusions can be drawn about the impact of leaky weirs and other NSF interventions on local hydrology and ecosystems. NSF is increasing in popularity. So, it is important to add to the understanding of its effectiveness. This will allow land managers to make more informed decisions about the appropriateness of certain interventions in specific climatic, geological, pedological and geomorphological contexts.

## 1.2 Scope

The scope of the project was limited to one-time sampling and analysis of surface and groundwaters along two transects that cross the Mulloon Creek, in the NSW Southern Highlands.

## 1.3 Aims and objectives

The overarching aim of this research is to build a conceptual model of water and salt movement through a floodplain, to assess the impact of leaky weirs on the connectivity of stream and groundwaters surrounding Mulloon Creek.

Objectives to achieve this aim are to:

1. Assess hydrologic connectivity by measuring hydraulic gradients and water quality parameters in the stream and groundwater, using piezometers installed along two transects up- and downstream of leaky weirs.
2. Perform stable isotope analysis of stream and groundwater to track the source and movement of water through the landscape.
3. Track the passage of dissolved salts by measuring and comparing major cations, anions and trace elements in water samples from surface and groundwaters along two transects.



## 2. Literature Review

### 2.1 Fluvial processes

River shape and stream flow dynamics are determined by the interaction between geology, topography, climate, biology, and human management practices (Bridge 2003). These complex relationships can be categorised into three linkage types. Longitudinal linkages refer to the relationship between upper and lower reaches of a stream, or between a trunk and its tributaries (Fryirs & Brierley 2013). Lateral linkages are the processes that connect a stream to its surrounding hillslopes and floodplain (Fryirs & Brierley 2013). Vertical linkages are the interactions between water and sediments at the surface and subsurface beneath the stream (Fryirs & Brierley 2013).

At different zones along a river system, sediment may be eroded, transported or deposited (Figure 2)(Fryirs & Brierley 2013). In a source zone, there is net erosion of sediment. These zones would normally be in the headwaters of a catchment. In a transfer zone, sediment enters and exits in roughly equal amounts. In accumulation zones there is a net import of sediment (Fryirs & Brierley 2013).

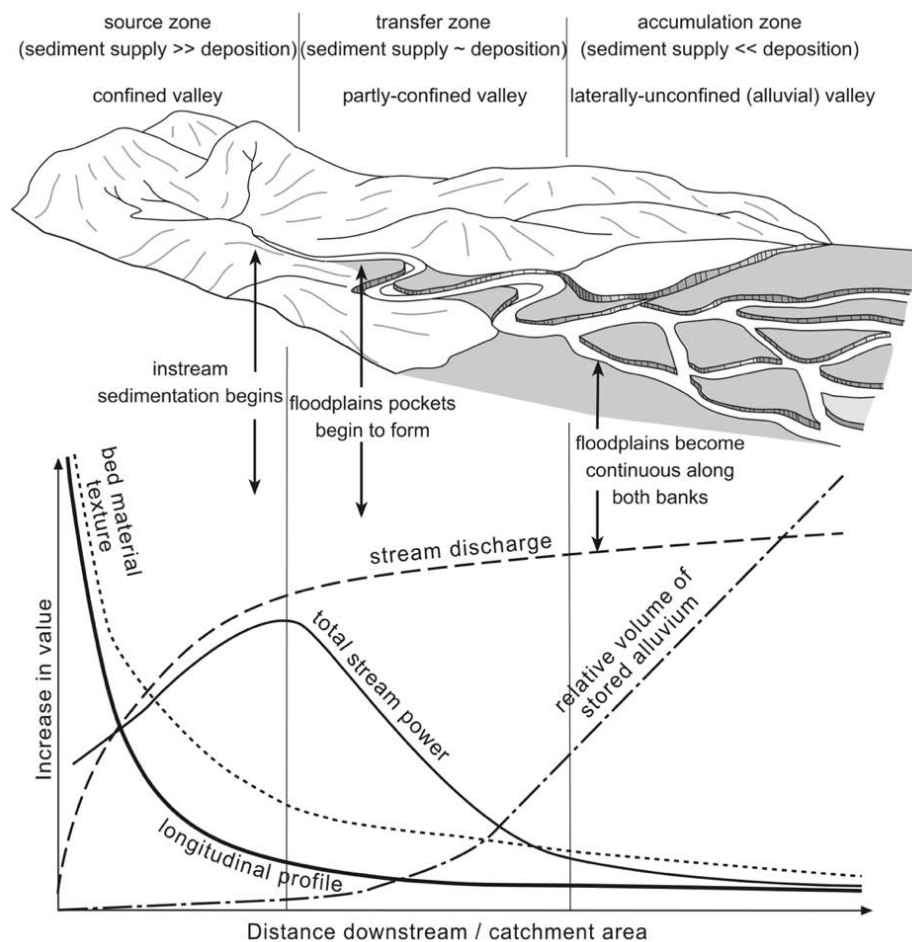


Figure 2: Diagram showing the depositional zones of a river in relationship to stream power, slope and discharge (Fryirs & Brierley 2013).

## 2.2 River types

Confined valley rivers are typically confined by steep slopes, a bedrock base and no floodplain, with high flow and significant sediment transport (Fryirs & Brierley 2013; Rhoads 2020). In wider valleys, usually at lower elevation, there is more potential for floodwaters to spread laterally, creating floodplains through sediment deposition. Wider floodplains also reduce the influence of bedrock on stream shape and flow (Fryirs & Brierley 2013). The shape, sinuosity and extent of braiding in streams is highly varied (Figure 4a).

Rivers that are laterally unconfined by surrounding geology may develop a continuous or discontinuous channel. These alluvial channels shape and are shaped by the water that flows through them and the amount of sediment they are transporting and depositing (Bridge 2003). These mutually reinforcing processes lead to complex channel evolution: sediment controls water flow, this flow regime then impacts sediment deposition and movement, which then once again changes flow conditions (Bridge 2003). A discontinuous alluvial river is known as a cut-and-fill system (Fryirs & Brierley 2013). In such systems, the stream undergoes periods of vertical sediment accretion, which fills the stream and inhibits water flow. This creates a wetland or swamp. Water pressure then builds, before incising a new channel through the existing alluvium (Figure 4b) (Fryirs & Brierley 2013). Rivers and streams with discontinuous channels occur in many parts of the world, and may be referred to as wetlands, swampy meadows, prairie potholes, beaver ponds, valley fills, mires, marshes or chains-of-ponds (Williams et al. 2020).

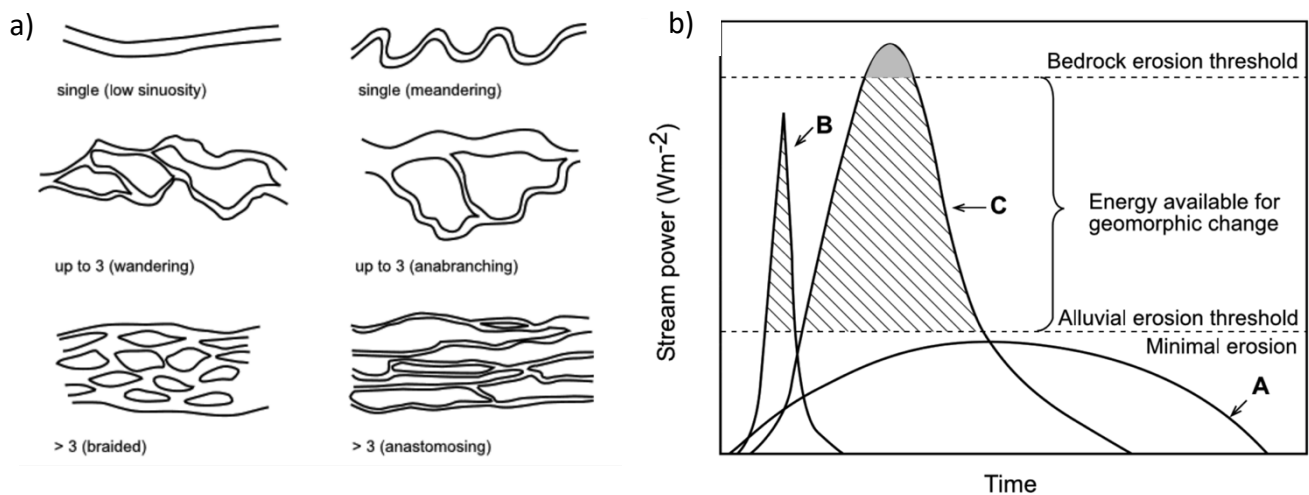


Figure 3: a) Various channel behaviours in alluvial systems, b) diagram showing the impact of stream power and time on alluvial and bedrock erosion (Fryirs & Brierley 2013).

The water table defines the boundary between aerated soil or rock and the saturated groundwater zone (Fryirs & Brierley 2013). The water table have an intermittent or permanent connection to surface waters (Section 3.4). The area of interaction, where both water and nutrients may be exchanged, is known as the hyporheic zone (Rhoads 2020). The extent of the hyporheic zone will depend on geology, stream characteristics, flora, water table height and topography.

### 2.3 Australian fluvial systems

Australia's ecological and fluvial systems are unique. These systems evolved as a result of the continent's dry climate, variable rainfall, ancient geology, relatively stable tectonics and flat topography, and the potential for prolonged periods of weathering and soil formation (Moore et al. 2018; Norris & Andrews 2010). These patterns are locally obscured, or overprinted in areas with high uplift and erosion, with associated higher energy landscape processes. In order for land management to be successful, these conditions must be understood. In particular, over millions of years, discontinuous watercourses, including chains-of-ponds, marshes and wetlands developed in Australia (Johnston & Brierley 2006). This is in contrast to the free-flowing rivers common in Europe and much of the rest of the world (Johnston & Brierley 2006). Evidence from geology as well as from accounts of early European settlers indicate that chains-of-ponds were found across Australia, commonly in wide valleys with low gradients (Hazell et al. 2003; Johnston & Brierley 2006; Mould & Fryirs 2017).

These wetland systems reduced the velocity and erosive potential of floodwaters (Norris & Andrews 2010) and performed a host of ecosystem services including: provisioning services, regulating services, cultural services and supporting services (Maltby & Acreman 2011; Norris et al. 2001). Chains-of-ponds are also an efficient and effective way of storing and moving water. Alluvial aquifers are reservoirs of groundwater that may connect to surface water streams. This greatly increases the residence time of water in the landscape. This buffering effect means streams would still flow during drought, as they would be fed from shallow groundwater (Fanning 1999; Somerville et al. 2006). In addition, riparian zones play an important role in filtering inflowing groundwater (Rassam et al. 2006). Plant roots trap fertility in the landscape, cycling nutrients in the terrestrial biosphere, rather than them being lost downstream. Chains-of-ponds systems potentially enable multiple landscape and ecosystem processes to occur: from the hyporheic and parafluvial zones, to the riparian zone, and extending across the floodplain (Goldman et al. 2017).

European understanding of the nature of Australian fluvial geomorphology was slow to develop. This was largely due to the difference between conditions on this continent compared to Europe and the Americas (Tooth & Nanson 1995). Human action may alter river conditions, specifically flow regime, via three major avenues: changed runoff; changed sediment configuration and changed vegetation assemblages (Fryirs & Brierley 2013). European land management from 1788 onwards has altered Australian watercourses through all three of these mechanisms. European graziers managed livestock the same way as was practiced in Europe. This degraded riparian vegetation, particularly reed beds of *Phragmites australis*, which previously slowed stream flow and kept floodplains hydrated (Norris & Andrews 2010). Incision and gully erosion often ensued (Figure 4) (Fanning 1999). In the Southern Tablelands and Highlands of NSW, more stream incision has occurred since

European settlement in the 1820s than at any other time in the Holocene record (Mould & Fryirs 2017). This removed the ability for the landscape to store moisture over time, simultaneously leading to more prolonged droughts and more damaging floods (Fanning 1999). The complexity of Australian river dynamics means confusion still persists over processes, and even names, of river types such as swampy meadows or chains-of-ponds wetland systems (Mactaggart et al. 2008).

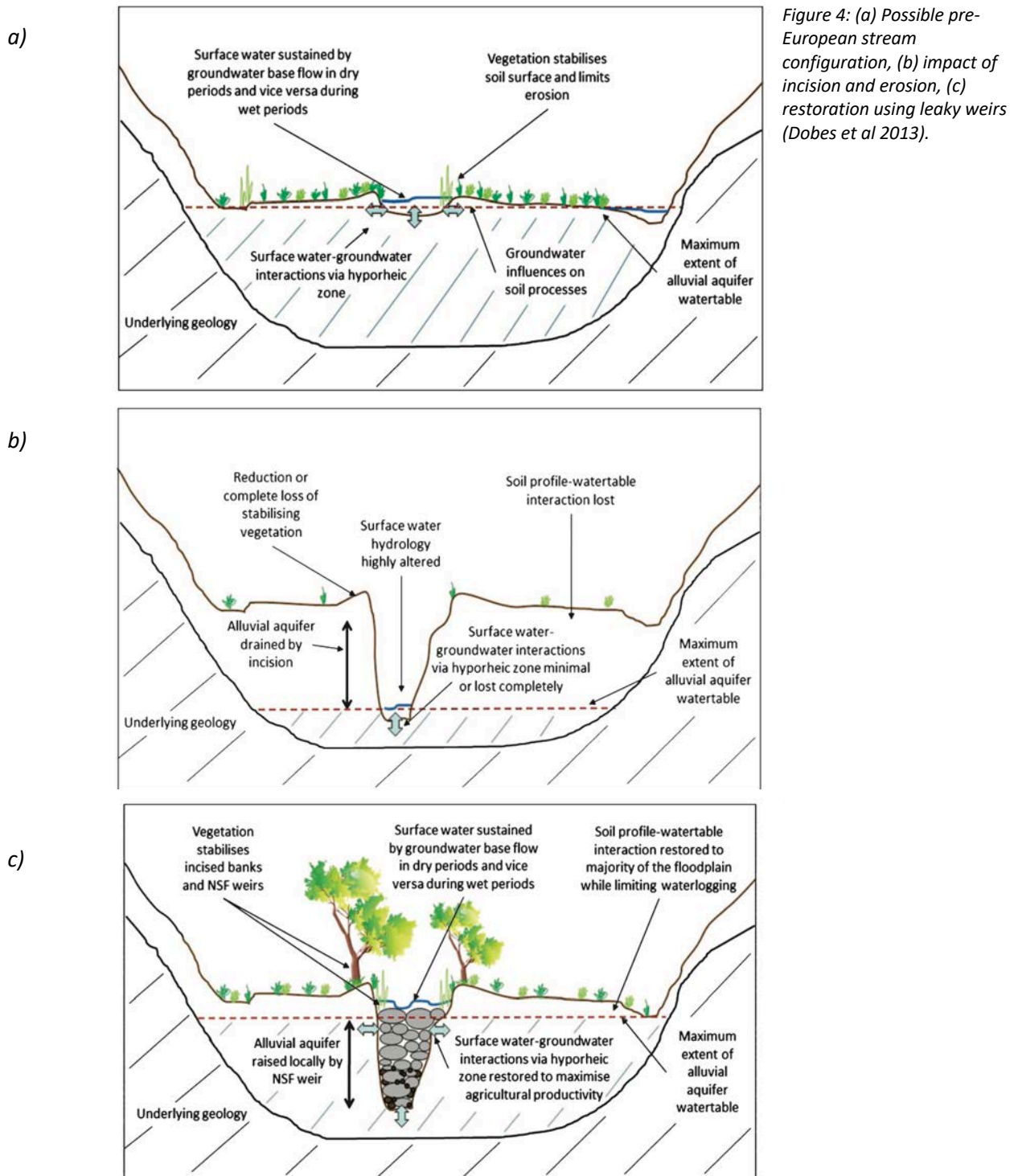


Figure 4: (a) Possible pre-European stream configuration, (b) impact of incision and erosion, (c) restoration using leaky weirs (Dobes et al 2013).

This impact of European land management on Australia river systems has been observed for decades (Hazell et al. 2003). However, the impact that a changing river structure has on ecology and landscape function has been consistently ignored or downplayed (Hazell et al. 2003). Healthy ecosystem function relies on adequate connectivity between surface and groundwaters (King et al. 2015), and the impact of altering trunk streams can have unpredictable higher order effects in other part of the catchment (Brierley & Fryirs 1999).

‘Natural’ or ‘healthy’ conditions for a river system are impossible to objectively specify. This is firstly because of the difficulty of seeing and measuring groundwater movements. In addition, there is an almost universal lack of knowledge about the nature of landscape hydrology from before European disruption. As such, it is important to experiment and test innovative and tailored land management strategies that show the potential to increase landscape function in a particular area. In this way, Australian rivers may be restored to a renewed, healthy state that fosters biodiversity and supports human economic resilience.

### **Salinity**

Increasing salinity is a major problem across Australian agricultural, urban and natural landscapes (Moore et al. 2018). Salinity levels are affected by the interaction between surface water, ground water, vegetation, soil and geology. Australia’s unique landscapes require novel management practices to function properly. The continent is prone to salinity problems due to the combination of its: a) dry and variable climate, b) flat topography and c) old, weathered geology (Moore et al. 2018). As management of the continent shifted from Indigenous Australians to early Europeans, landscape function deteriorated. In particular, salinity increased in many agricultural areas. In part, this was caused by native deep-rooted perennial plants being replaced by shallow-rooted annual grasses and crops (Banks et al. 2011). This shifts the balance between surface and groundwaters, which can cause mobilisation of salts in the shallow regolith.

Salinity occurs in three major ways (Moore et al. 2018):

1. Land salinity, which occurs when there is a high water table, leading to evaporation at the soil surface, and an increase in salt concentration. This leads to reduction in vegetation, and hence erosion.
2. In-stream salt load, a rate measurement that measures the mass of dissolved salt in a stream over time. Irrigation using stream water with high in-stream salt load can lead to irrigated soils becoming unviable.
3. In-stream salt concentration, measured by electrical conductivity (EC). Increasing EC can dramatically affect fresh-water ecosystems and reduce landscape function.

The interplay of these three types of salinisation combined with ecological and hydrological processes creates complex outcomes in the landscape. Misunderstanding of these processes has previously led to incorrect management and remediation strategies to be implemented

(Moore et al. 2018). In response, Moore et al. (2018) proposed the Hydrogeological Landscape (HGL) framework – a holistic strategy for assessing the cause of salinity in an area of land and devising a management regime to improve conditions in that location. The HGL technique involves identifying contiguous parcels of land that are impacted by a certain salinity process. This compartmentalisation then makes it possible to implement the interventions that are relevant for a certain area (Jenkins et al. 2010d). Understanding the relationship between surface and groundwaters in a given area is crucial for limiting increases in salinity and ensuring sustainable agricultural production (Somerville et al. 2006).

Most research into stream-aquifer connectivity focusses on local-scale interaction. One example of catchment-scale research is a study of the Rocky River Catchment on Kangaroo Island, South Australia (Banks et al. 2011). Researchers combined hydrochemical, hydraulic and tracer techniques to build a coherent picture of water movement between aquifers and streams. Surface and groundwaters were sampled from piezometers and streams over a 28-month period. Physicochemical properties including salinity were measured *in situ*, and samples were collected to measure strontium isotope ( $^{87}\text{Sr}/^{86}\text{Sr}$ ) ratios, and cations and trace element proportions. Results show an increase of EC and all major ions in river water as elevation decreases. The researchers hypothesise that this increase in salinity is caused by evapotranspiration coupled with discharge of more saline shallow perched aquifers into streams. This implies that land-use change and clearing of vegetation can have significant impacts on the state of connectivity between ground and surface waters.

#### 2.4 Groundwater: composition, movement and measurement

The health of Australian landscapes is dependent on a connection between surface and groundwater (Banks et al. 2011). When this connection is severed, a positive feedback loop of erosion, drying and aridification can be set in motion (Banks et al. 2011). To observe the extent of ground-surface water interaction, a combination of physical, ecological, hydrometric, hydrochemical and hydrogeological indicators should be measured. Remote sensing and modelling may also provide insight (Brodie et al. 2007; Ransley et al. 2007). Despite the importance of understanding landscape hydrology, land managers may neglect monitoring because of the perceived difficulty (Ransley et al. 2007).

For *in situ* measurement of groundwater, piezometers are installed to specific depths according to the configuration of aquifers. To assess the interaction between stream water and aquifers, the piezometer will normally be placed along transects that are oriented perpendicular to the axis of the valley, along a toposequence. This based on the assumption that the orientation of groundwater flow is somewhat similar to the surface runoff flow direction. The ideal placement would be in the direction of groundwater flow, but this is difficult to evaluate until the piezometer array is in place (Figure 5) (Brodie et al. 2007;

Sophocleous 2002).

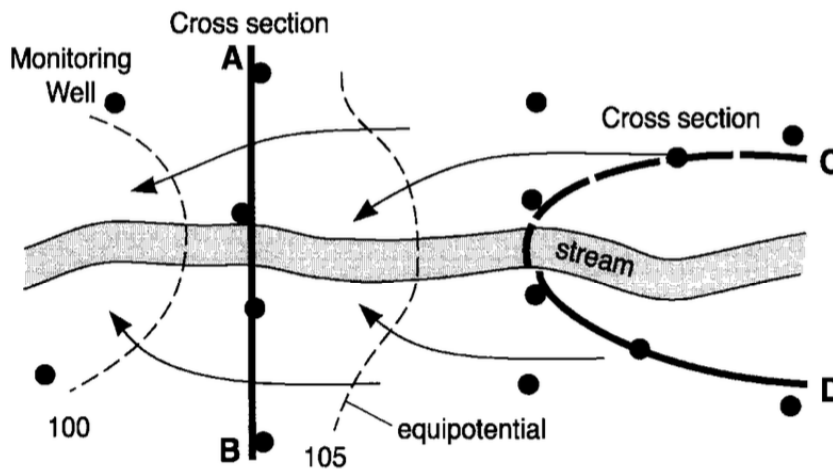


Figure 5: Two layouts of piezometer cross-sections. Transect AB does not follow a groundwater flow line; CD does (Sophocleous 2002).

The exchange of water between stream and aquifer at a large scale is governed by a) the hydraulic conductivity of stream sediment and surrounding soil and geology, b) the relative height of stream stage and groundwater levels and c) the position of the stream through the geology of the surrounding alluvial plain (Sophocleous 2002). Hydraulic conductivity is a function of the connectivity, permeability and transmissivity of surrounding regolith and geology, and the viscosity of the water.

The amount and direction of water movement between stream and aquifer may be inferred by assessing hydraulic gradients across a floodplain, using Darcy's Law:

$$Q = A \frac{dh}{dl} K \quad \text{Equation 1}$$

Where:

- Q is the flux of water,
- A is the cross-sectional area,
- dh is the change in vertical distance,
- dl is the change in horizontal distance and
- K is the hydraulic conductivity (constant of proportionality).

All hydrometric methods rely on the accuracy of K, the true value of which can vary greatly, even across small areas (Brodie et al. 2007). As such, these measurements have varying degrees of accuracy and usefulness.

Groundwater hydrographs can be used to assess the direction of groundwater flow. Combining this data with stream levels gives a hydraulic gradient between water table and stream (Brodie et al. 2007). The presence or lack of a hydraulic gradient differential does not

necessarily prove connectivity between the two water sources. But this gradient can be used to infer the most likely state of connectivity.

A stream is connected to its surrounding groundwater if it is either feeding or being fed by the groundwater; there may or may not be an unsaturated zone separating surface and groundwaters (Reid et al. 2009). If a stream is gaining, it will be receiving some portion of its water from the aquifer (Figure 6a). If the stream is losing, it will feed water to the aquifer. This may occur in a state of saturated or unsaturated connection (Figure 6b, c). Bank storage will occur when stream water enters the banks above the prior water table, such as during a storm (Figure 6d). This water will then re-enter the stream within days or weeks.

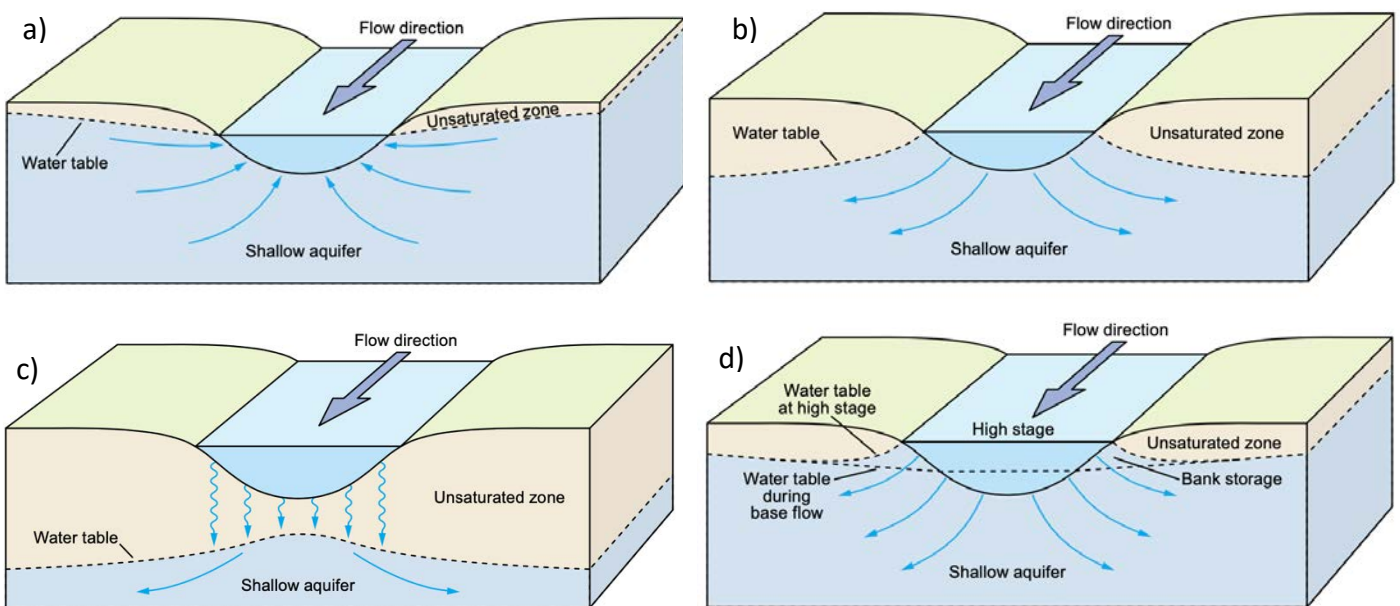


Figure 6: Diagrams representing different relationships between a stream and surrounding groundwater: a) gaining stream; b) losing stream with no unsaturated zone separating stream and aquifer; c) losing stream with unsaturated zone; d) losing stream with bank storage (Reid et al. 2009).

The amount of water that flows through or is stored in a water body can be calculated using a water budget equation (Healy 2010). This technique relies on the concept of mass conservation to sum the various inflows and outflows of a water body over a given time period (Healy 2010). In the case of a floodplain aquifer, the following equation may be used:

$$\Delta S = G_{in} - G_{out} + Q_{in} - Q_{out} + P - ET - A \quad \text{Equation 2}$$

Where:

- $\Delta S$  is the change in the amount of water stored in the groundwater system,
- $G$  is the groundwater in- and outflow,
- $Q$  is the surface water in- and outflow,
- $P$  is the precipitation inflow,
- $ET$  is evapotranspiration from groundwater, and
- $A$  is the abstraction of water from the system by humans, such as by pumping.



All terms are volumetric rates per unit area, e.g. mm/yr (Healy 2010).

#### 2.4.1 Water stable isotope analysis

Analysing ratios of H and O isotopes in water molecules is an effective method for tracing water movement through landscapes (Cook & Herczeg 2012). This analysis is useful because H and O rarely react chemically at ambient temperatures, while they are affected by phase changes in water (Short 2017). The most common ratios measured are  $^2\text{H}/^1\text{H}$  and  $^{18}\text{O}/^{16}\text{O}$  (Cook & Herczeg 2012). Ratios in samples are measured not in absolute terms, but in relative terms in comparison with a standard, most commonly the Vienna Standard Mean Ocean Water (VSMOW) standard (Cook & Herczeg 2012). Delta notation is used to represent these ratios in parts per mil (‰) (Cook & Herczeg 2012). The expression for stable isotope notation is:

$$\delta_x = \delta_{x\text{-std}} = \left[ \frac{R_x}{R_{\text{standard}}} - 1 \right] \times 1000 \quad \text{Equation 3}$$

Where  $R_x$  is the sample ratio of  $\delta^{18}\text{O}$  or  $\delta^2\text{H}$ , and  $R_{\text{standard}}$  is VSMOW.

Differences in isotopic ratios arise because physical processes affect molecules of varying mass to different extents (Cook & Herczeg 2012). For example, heavier molecules will evaporate proportionally less frequently than lighter molecules. The inverse is true in the case of precipitation. Deuterium ( $^2\text{H}$ ) excess is a quantity used to assess how  $^2\text{H}$  is being separated from  $^{18}\text{O}$  (Cook & Herczeg 2012). A high deuterium excess means water has undergone relatively less evaporation than water that has a lower deuterium excess, because the  $^{16}\text{O}^2\text{H}^1\text{H}$  molecule is lighter than  $^{18}\text{O}^2\text{H}^2\text{H}$ , so it evaporates first (Figure 7) (Cook & Herczeg 2012). So, the  $^{16}\text{O}^2\text{H}^1\text{H}$  molecule can only exist in waters that have not undergone a lot of evaporation. These different processes and conditions produce predictable isotopic changes, which were outlined by Rayleigh (1896)(Figure 8). The general equation for deuterium excess is:

$$\text{Deuterium excess} = \delta^2\text{H} - 8 \cdot \delta^{18}\text{O} \quad \text{Equation 4}$$

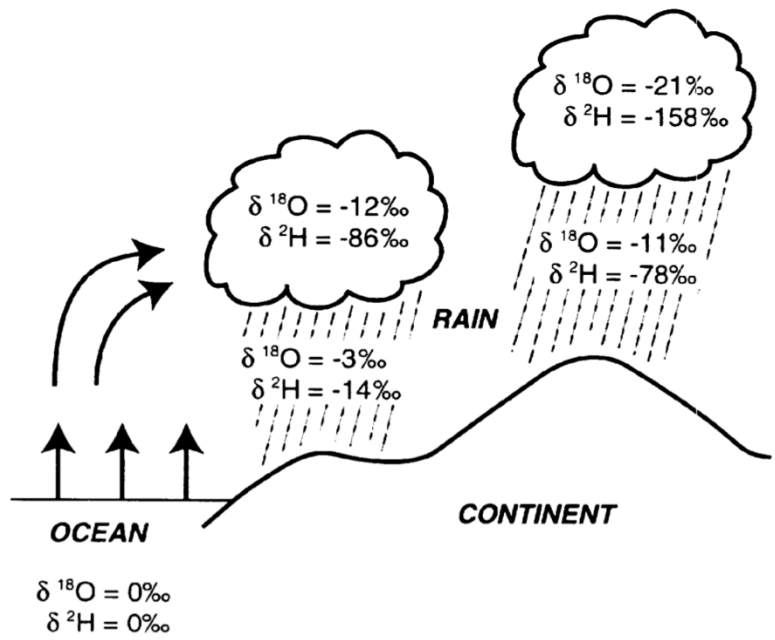


Figure 7: Rayleigh fractionation of water molecules according to isotopic makeup, as a result of climatic phenomena (Cook & Herczeg 2012).

The mean worldwide relationship between  $\delta^{18}\text{O}$  and  $\delta^2\text{H}$  is referred to as the Global Meteoric Water Line (GMWL), with a deuterium excess of 10.8 (Cook & Herczeg 2012). However, the deuterium excess will vary between areas. These local equations are referred to as Local Meteoric Water Lines (LMWLs) (Cook & Herczeg 2012).

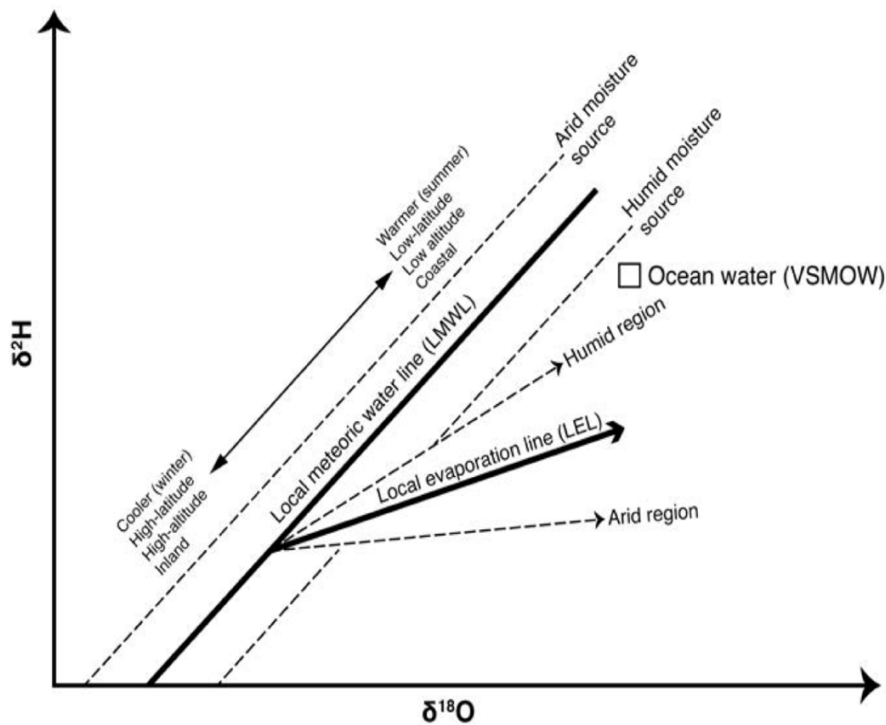


Figure 8: Diagram showing the impact of hydrologic and climatic processes on isotopic ratios in water (Short, 2017)

Short (2017) collected rain, creek and groundwater samples from the Lake George Basin, NSW. A LMWL was constructed from the  $\delta^{18}\text{O}$  and  $\delta^2\text{H}$  values of the rainwater samples, using a precipitation amount weighted reduced major axis (RMA) regression. The LMWL has a slope of 7.8 and deuterium excess of 13.3, giving an elevated line with shallower slope compared to the GMWL (Figure 9a). The groundwater line of best fit (Figure 9a) suggests that groundwater has undergone evaporation during the recharge process. Short also plotted isotopic ratios against depth, for groundwater samples collected in cores beneath Lake George (Figure 9b). This led to the hypothesis that groundwater infiltration into the Lake is mixing with fresh lake water from above, which provided insight into past “drying phases” and “filling phases” in the lake.

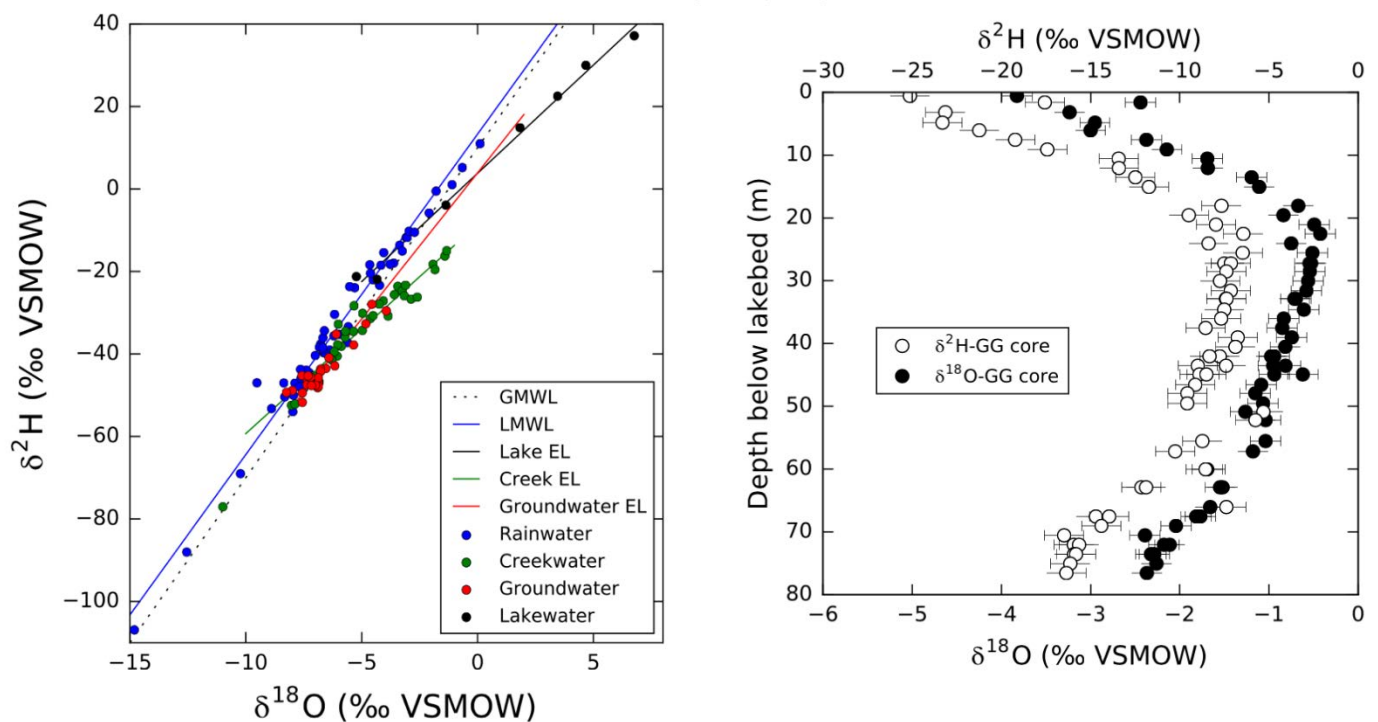
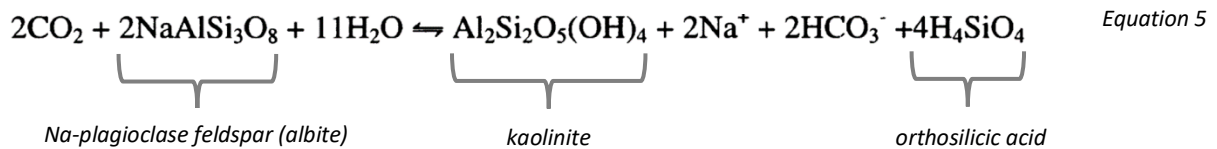


Figure 9: a) Stable isotopes of rain, surface and groundwaters in the Lake George area, b) stable isotopes according to depth, from porewater from underneath Lake George (Short 2017).

#### 2.4.2 Geochemical processes

The dissolved chemical components of groundwater are primarily the cations  $\text{Na}^+$ ,  $\text{K}^+$ ,  $\text{Mg}^{2+}$ ,  $\text{Ca}^{2+}$  and anions  $\text{Cl}^-$ ,  $\text{SO}_4^{2-}$  and  $\text{HCO}_3^-$  (Hiscock 2014). These ions mainly originate from precipitation or mineral weathering (Cook & Herczeg 2012). The interaction of rainwater with soil  $\text{CO}_2$  forms carbonic acid. This dilute acid together with other organic acids produced in the soil zone can drive the release of cations and produce  $\text{HCO}_3^-$  ions through dissolution of carbonate and silicate minerals (Cook & Herczeg 2012). Primary silicate minerals (e.g. Na-Plagioclase feldspar) weather to form clays by the following reaction (Berner & Berner 1987; Cook & Herczeg 2012):



In this reaction, the unstable albite forms the more stable kaolinite after reacting with carbonic acid. Na cations and HCO<sub>3</sub><sup>-</sup> are released into solution, producing a Na-HCO<sub>3</sub> type fluid. The silica that is also produced during this reaction is the main source of groundwater silica (Cook & Herczeg 2012). As a result of these and other reactions, groundwater may evolve greater Total Dissolved Solids (TDS) than stream water. The manifestation of salt is enhanced by evapotranspiration, which removes excess water causing ions to concentrate. Cation exchange is another important interaction between groundwater and the surrounding geology. Clay particles are negatively charged, meaning they attract cations, which adsorb onto the clay particles, shifting ionic concentrations in water.

Cartwright and Morgenstern (2016) studied stream-groundwater interaction of a chain-of-ponds system along Deep Creek, a tributary of the Maribyrnong River in central Victoria. They found strong overlap between chemistry of river and groundwater (Figure 10). In the surface water, Na made up 67–77% of cations and Cl was 58–90% of anions. In the groundwater, Na was 57–78% and Cl 48–69% (Figure 10). The authors use this evidence to build a case that the stream and the aquifer are connected. Specifically, that the stream seems to be receiving inflow from the groundwater.

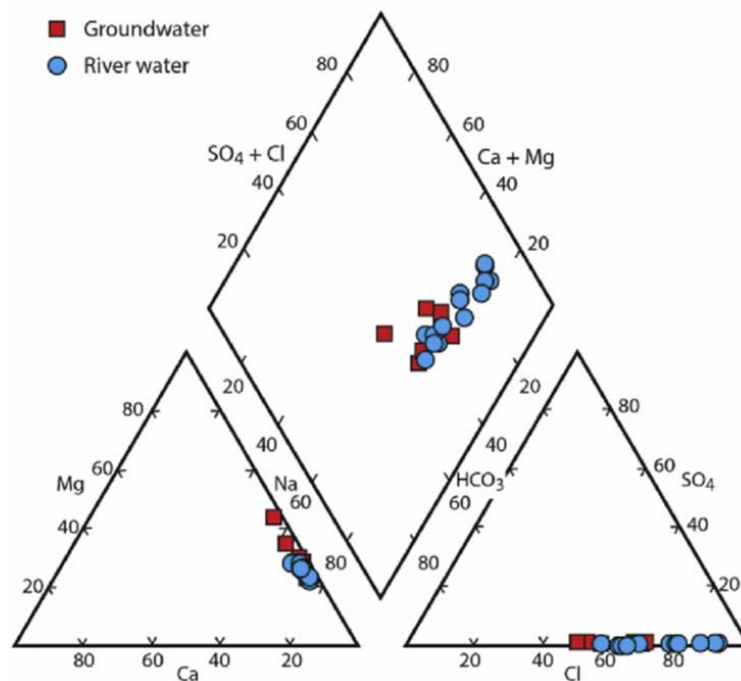


Figure 10: Piper diagram showing major ion molar ratios of river and groundwater in and around Deep Creek, Victoria (Cartwright & Morgenstern 2016).

Gray et al. (2019) sampled surface waters in the Upper Murrumbidgee Catchment of NSW and ACT. Samples were plotted on Piper diagrams according to the outcrop geology, including the same two geologies that are present in the present study site: Silurian granite and Ordovician metasediments (Figure 11). Surface waters were Na-Ca-Mg-HCO<sub>3</sub> types with some Na-Ca-Mg-Cl type.

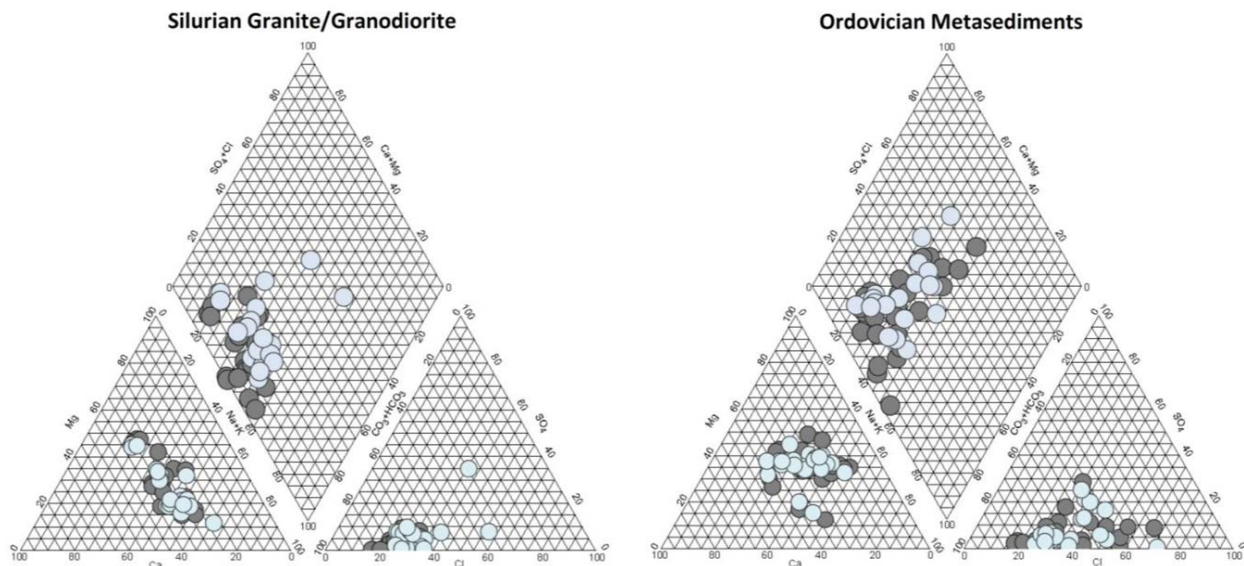


Figure 11: Piper plots of surface water samples from the Murrumbidgee River, separated by outcrop geology. Darker circles collected in November/December 2018, lighter circles in April 2019 (Gray et al. 2019).

Inorganic ions are often used to trace water movement through aquifers (Cook & Herczeg 2012). Chloride is a common inorganic mineral tracer for several reasons. Chloride is not found in most common rock forming minerals, so it is not usually involved in mineral precipitation or dissolution reactions (Cook & Herczeg 2012). Neither is it electrostatically attracted to the aquifer rock matrix (Cook & Herczeg 2012). The Cl molecule is highly mobile and moves through an aquifer in a similar manner to water (Cook & Herczeg 2012). Precipitation is the primary source of Cl in ground and surface water. When evapotranspiration occurs, Cl remains in the soil water solution. When the water leaves the root zone and enters the aquifer, it carries this enriched salt signature with it (Cook & Herczeg 2012). If evaporation is the only chemical process occurring, the ratio of Cl to other ions will stay consistent as Cl concentration changes. By plotting other ions against Cl, it is possible to analyse whether there is relative enrichment or depletion of those ions as waters become more saline. In this way, a model can be developed that explains processes of salt addition, such as cation exchange and mineral dissolution, or salt removal by mineral precipitation.

Short (2017) analysed water types in the Lake George area and compared ratios of Cl/Br (Figure 12). The large variation in rainwater Cl/Br ratios found implies that rainfall in this area fluctuates seasonally and is brought in by different coastal and inland weather systems.

The Lake George samples are tightly clustered and are more similar to groundwater rather than the surface water from five creeks that drain into the Lake. This suggests that groundwater is the dominant source of lake water

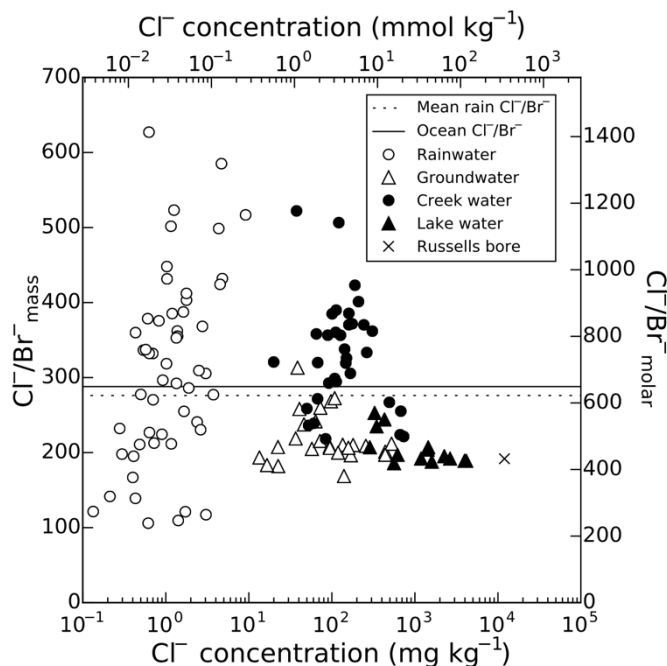


Figure 12: Cl/Br ratios plotted against Cl concentration for various water sources in the Lake George Catchment (Short 2017).

Somerville et al. (2006) measured major anions in ground and stream water around Widden Brook, a tributary of the Goulburn River in the Hunter Valley NSW. The study found that the  $\text{HCO}_3^-/\text{Cl}^-$  ratio was mostly much greater than 1, which is higher than seawater. This implies that ions in groundwater and stream water came from water-sediment reactions and not from aeolian deposition. Concentrations of ferrous iron ( $< 1 \text{ mg/L}$ ) and sulphates ( $< 5 \text{ mg/L}$ ) in the alluvial floodplain groundwater was much lower than the concentrations in floodplain terrace groundwater ( $17 \text{ mg/L}$  and  $> 10 \text{ mg/L}$ ). Further, stream chemistry and salinity differed from groundwaters and also varied along the length of the stream. The authors note that the large differences between nearby water sources has implications for future land management. At the time of publication of this research, there were proposals to install leaky weirs at points along Widden Brook. The authors suggest this may mobilise salts from the floodplain terraces and thereby increase salinity in the stream. It is important to consider such impacts before recommending widespread use of leaky weirs.

### 2.5 Natural Sequence Farming

Anecdotal evidence suggests that NSF interventions can have positive impacts on hydrology and fertility in agricultural land. But the whole-of-landscape approach advocated by NSF practitioners means it is difficult to assess the impact of one intervention or variable in isolation. There have been few studies published that attempt to quantify the impact and validity of NSF. Weber and Field (2010) compared NSF sites paired with adjacent conventionally managed agricultural land with comparable geomorphology. They found

improvements across several variables. For NSF total phosphorous was 938.59 ppm compared to 827.19 ppm in the non-NSF sites. Soil effective cation exchange capacity was 34.54 cmol/kg at the NSF sites versus 29.58 cmol/kg on non-NSF sites. Abundance and diversity of macrobiota were also higher in the NSF sites.

Hickson (2017) studied the impact of NSF interventions at the Home Farm property on Mulloon Creek, NSW, which has been under NSF-style management since 2006. In some areas surrounding NSF leaky weir construction, a statistically significant increase of 0.37 m in the height of the water table was measured one year after leaky weirs were installed (Table 1). However, aquifer recharge was found to be highly dependent on aquifer sedimentology. Where clay units dominated near the surface, infiltration was restricted and there was less or no rise in the water table.

Table 1: Comparison of groundwater levels before and one year after the installation of leaky weirs along Mulloon Creek (Hickson 2017).

Early Period		Late Period	
Mean elevation (m)	728.49	Mean elevation (m)	728.71
Elevation StDev.S (m)	2.60	Elevation StDev.S (m)	2.41
Elevation Var.S (m)	6.78	Elevation Var.S (m)	5.79
Mean depth (m)	2.10	Mean depth (m)	1.73
Depth std dev (m)	0.73	Depth std dev (m)	0.75
Depth variance (m)	0.54	Depth variance (m)	0.56

At some sites on the Home Farm, Hickson hypothesised that increasing hydrostatic pressure in stream waters via installation of leaky weirs would not generate enough potential to influence the recharge of higher-elevated mid-slope aquifers. Overall, Hickson hypothesised that for NSF management techniques to be most effective, a) a floodplain requires porous sedimentary units and aquifers that are not already at capacity, and b) there must be adequate pathways to link stream water with groundwater. On the Home Farm at Mulloon Creek, these conditions are met. However, in the Lower Mulloon area (which is the site for

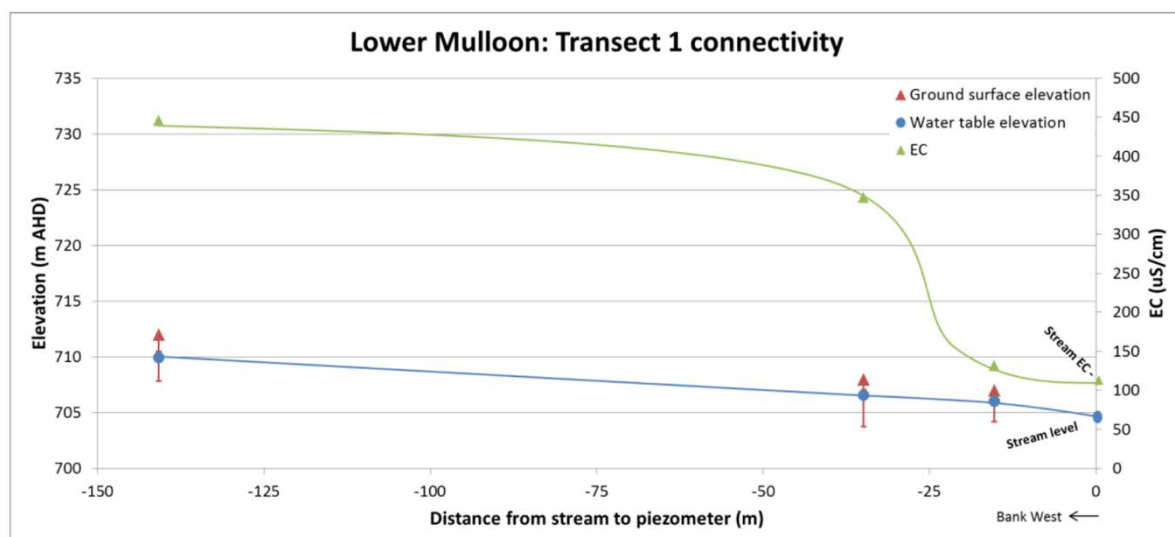


Figure 13: Hydraulic potential and electrical conductivity along a transect at Lower Mulloon, from Hickson (2017). This transect is upstream and south of the present research study site.

the present study), these conditions were not met. On one transect at Lower Mulloon, EC measurements implied a connection between creek and shallow groundwater, but only up to 25 m from the creek. After which, EC rapidly doubled before finding a new equilibrium (Figure 13; Hickson 2017). These findings emphasise the importance of only using rehabilitation techniques that fit the context of a particular area.

Keene et al. (2007) studied the impact of a leaky weir on the stream and alluvial aquifers around Widden Brook, NSW. The channel has a sandy bed and has been significantly degraded and incised. Four transects of piezometers were installed to a depth of 4 m across the floodplain, orthogonal to the stream. Over a one-year period, in-field measurements were carried out, and samples collected for chemical analysis. It was found that stream water had much higher dissolved oxygen than groundwater. Groundwater also tended to be more saline. The EC of groundwater closer to the leaky weir tended to mirror that of stream water (Figure 14). Groundwater EC increased with distance from the leaky weir, suggesting hydrological exchange occurring at the weir caused the reduction in nearby EC.

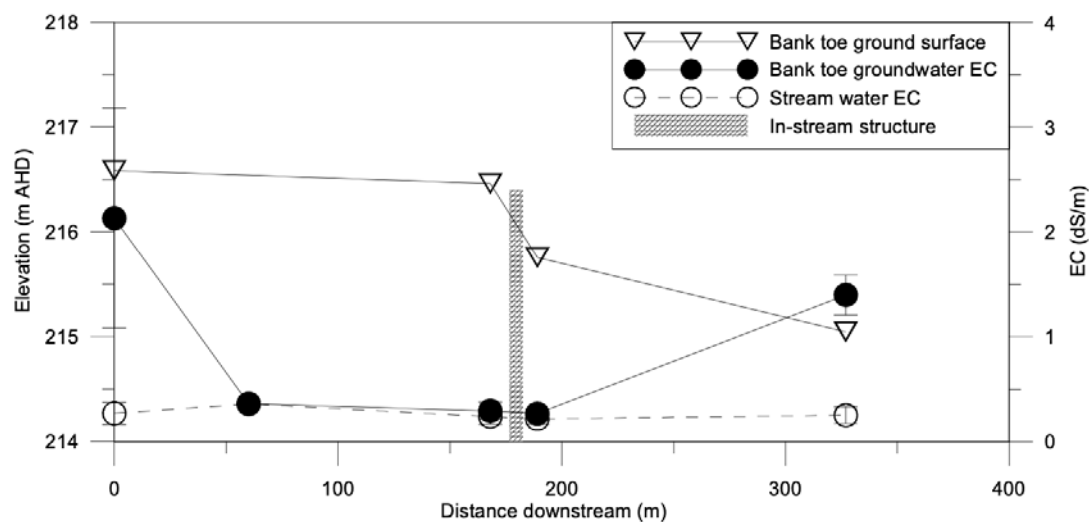


Figure 14: Longitudinal profile of leaky weir in Widden Brook, showing topographic elevation and EC of stream and groundwater (Keene et al. 2007).

Streeton et al. (2013) studied the impact of the installation of leaky weirs in rangelands in the Spring Creek catchment, NSW. Soils were sodic, making the stream more susceptible to erosion. The same conditions are present at the Mulloon Creek study site. The rehabilitation works at Spring Creek included fencing to keep stock away from stream banks, revegetation, and the installation of 13 leaky weirs constructed from 0.9 m blocks of local basalt. Rehabilitation was tracked for five years. Testing was mainly carried out on stream deposits and floodplain soils; aquifer connectivity was not a focus of the research. The authors noted that prior to the construction of leaky weirs, stream incision had increased longitudinal connectivity of the stream, increasing the flux of water and sediments down the channel. Once the leaky weirs were installed, sediment aggradation increased significantly, with aggradation at the weir sites averaging 3 mm/yr in the first two years after installation, and



15 mm/yr by the fifth year. Significant improvement in riparian vegetation condition was also reported.

Leaky weirs will only cause sediment aggradation if the upstream catchment is collecting and transporting sediment to the weir's location. If the stream does not have a sediment source, the weir may have limited effect fertility build-up. Further, weirs constructed in areas with sodic soils will require frequent monitoring and maintenance to ensure highly erodible soil and sediment does not erode around the edges of a weir, creating a new channel. New South Wales and Australian Capital Territory Regional Climate Modelling (NARCLiM) suggests rainfall events will become more sporadic but higher intensity in the future (Evans et al. 2017). In such a case, sediment held back by weirs may be easily entrained and eroded again when large flood events overtop the weir.

### 3. Study Area

Mulloon Creek sits within a 400 km<sup>2</sup> sub catchment of the Upper Shoalhaven River in the NSW Southern Highlands (Figure 15) (Johnston & Brierley 2006). The climate is temperate subhumid to humid, with average rainfall of 636 mm (Figure 16) (Bureau of Meteorology 2021b; Johnston & Brierley 2006). Elevation at the study site is 690 to 720 m AHD (NSW Government Spatial Services 2015).

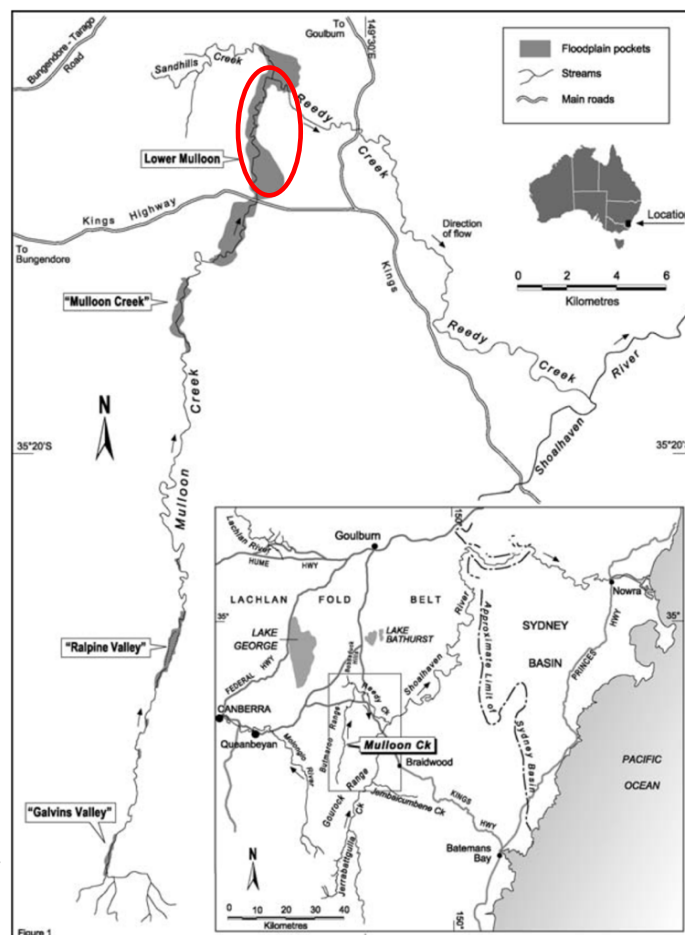


Figure 15: Regional setting of Lower Mulloon with study site highlighted (Johnston & Brierley 2006).

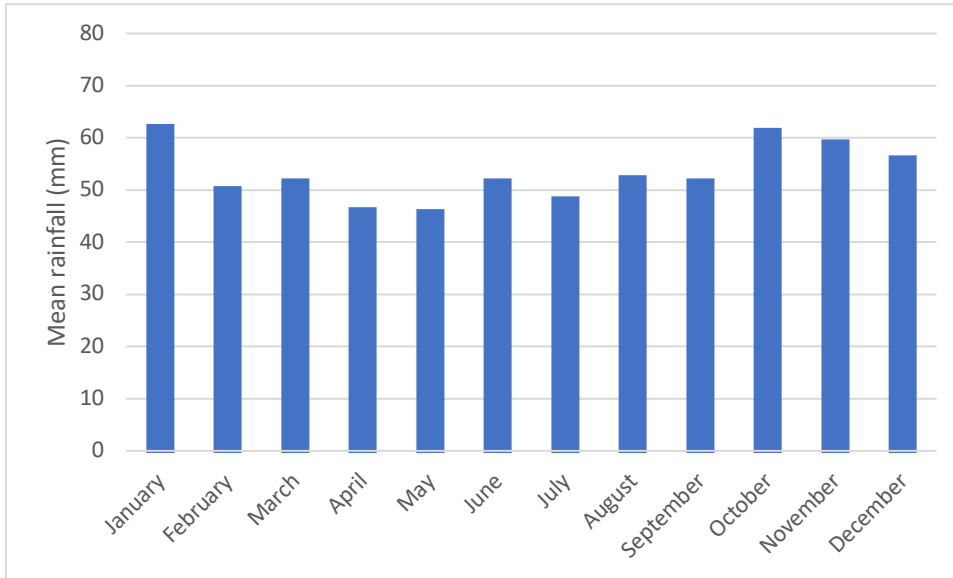


Figure 16: Bungendore Post Office average monthly rainfall, 1890–2021 (average annual rainfall: 635.5 mm) (Bureau of Meteorology 2021b).

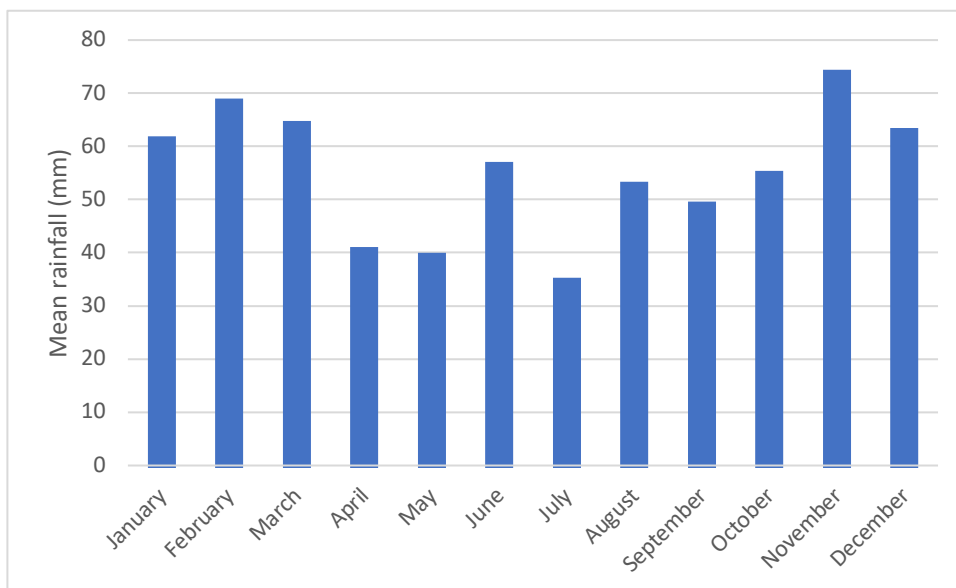


Figure 17: Braidwood racecourse average rainfall, 1985–2021 (average annual rainfall 636.7 mm) (Bureau of Meteorology 2021a).

Mulloon Creek is broken up into distinct floodplain pockets, resembling ‘beads on a string’, with bedrock separating and confining each distinct pocket (Johnston & Brierley 2006). The study area is a floodplain pocket at the downstream end of Mulloon Creek, referred to as Lower Mulloon (Figure 15). The floodplain extends up to 1 km in width, along a 10 km reach of the Creek (Figure 18).

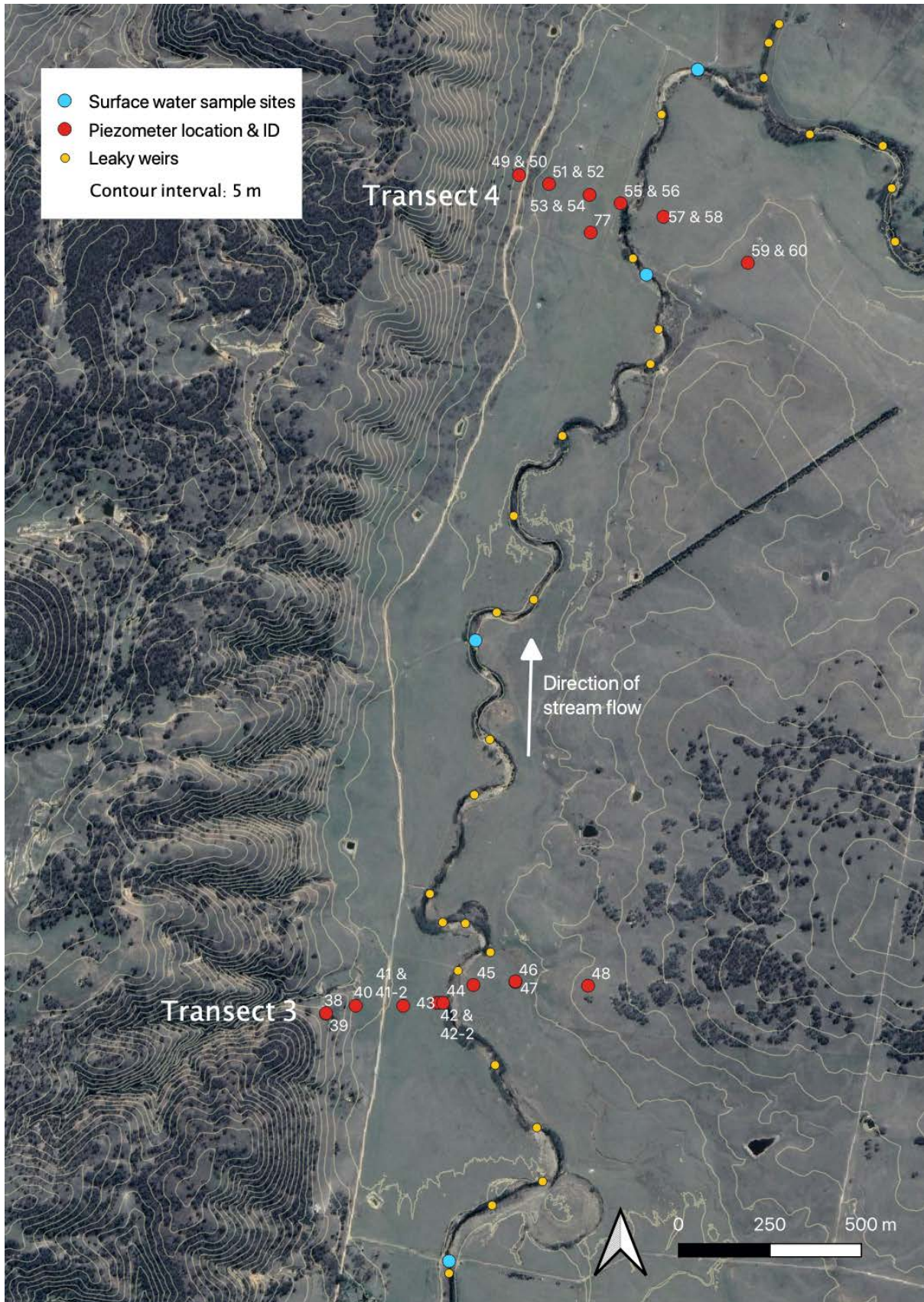


Figure 18: Sampling sites and leaky weir locations along the Lower Muloon Creek floodplain.

The Mulloon area lies in the Lachlan Fold belt, with underlying rocks dating of Paleozoic age (570 to 225 Ma; (Jenkins et al. 2010c). The study site is an incised alluvial floodplain, with an upfaulted horst block of Ordovician metasediments to the west and a pale-coloured granite (leucogranite) member of the Siluro-Devonian Boro Granite forming low hills, with crestal exposures, to the east (Fitzherbert et al. 2017; Jenkins et al. 2010c). The Mulwaree Fault escarpment on the western side of the study area rises steeply above the Mulloon Creek alluvial terraces and floodplain. The basement geology is Ordovician (479.4 Ma to 458.4 Ma) marine metasediments (turbidites) of the Abercrombie Group (Colquhoun et al. 2020; Gray & Foster 2004; Jenkins et al. 2010a). These metasediments are dominated by interbedded, folded and cleaved sandstone, siltstone and shale with minor greywacke, and pockets of sulphidic black shale and chert (Colquhoun et al. 2020; Jenkins et al. 2010a). The rocks are incipiently metamorphosed and have weathered to form skeletal soils (lithic tenosols) (Jenkins et al. 2010a). Colluvial transport of weathered rocky sediment during the Quaternary (2.58 Ma to present) formed a bench-like piedmont landform at the base of the fault escarpment. The piedmont is an accumulation of colluvium that has been eroded from the flanks of the adjacent range, deposited due to slope processes along a vector perpendicular to the direction of the stream flow.

Soils on the west are lithic tenosols on the crests and upper slopes; yellow and red rudosols on the upper to mid slopes; brown to red chromosols on the mid to lower slopes; brown podosols on the alluvial terraces and flood plains; and localised swampy areas of organosols and sodosols along the Creek line (Department of Planning 2021). Soils on slopes show a distinct textural contrast between A and B horizons. The B horizon typically has low soil pH and is commonly high in Mg, Ca and Al (Isbell 2016). On the crests and flanks of the range the regolith is thin, around 30 cm (Jenkins et al. 2010a). Quartzose clayey sands dominate, with kaolinite the dominant clay species (Jenkins et al. 2010a). Significant groundwater flows occur laterally through the porous colluvium and along fracture lines in the deeper sandstone basement rock, recharging groundwater systems (Jenkins et al. 2010a).

To the east of Mulloon Creek is the Siluro-Devonian (410.8 Ma to 407.6 Ma) Boro Granite, originating from a magma intrusion into the Ordovician metasediments in the late Silurian to early Devonian (Colquhoun et al. 2020). Processes of compression, uplift and erosion brought the granite to the surface. The granite regolith is quartzose-sand-rich with thick (<5m) profiles (Jenkins et al. 2010b). If salts have naturally accumulated across this landscape through geological time, then a thicker regolith veneer presents a greater potential salt store in the landscape (Moore et al. 2018). Aquifers are unconfined in unconsolidated regolith and jointed and faulted fractured leucogranite (Jenkins et al. 2010b).

Approximately 12,000 years ago, the proto-Mulloon Creek began to accumulate gravelly sediment, causing vertical accretion, channel discontinuity and formation of swampy



meadows and chains-of-ponds (Figure 19) (Johnston & Brierley 2006). This sediment originated upstream in the headwaters of Mulloon Creek. These headwaters have a similar geology of Ordovician metasediments and Siluro-Devonian granite (Colquhoun et al. 2020). Periods of different flow conditions created alluvial flood plains which today form a sequence of successive alluvial terraces adjacent to the contemporary Creek.

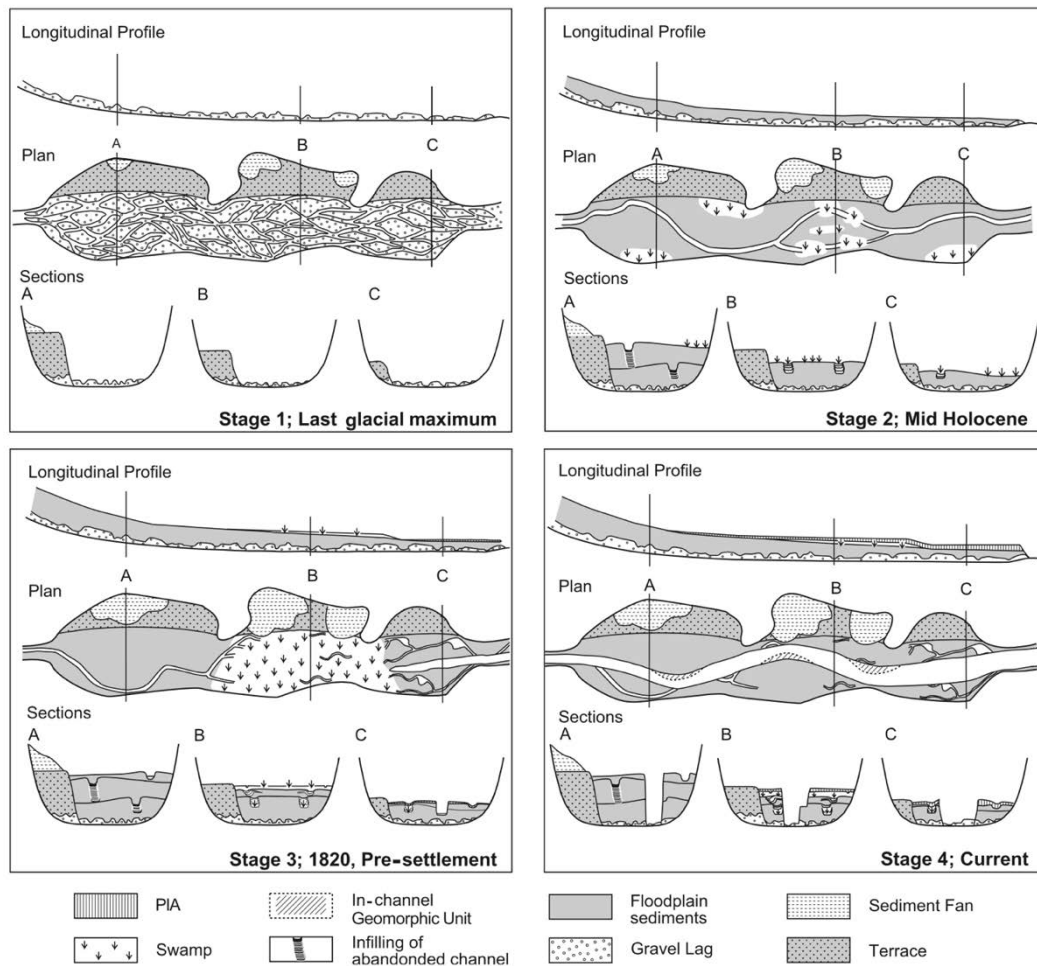


Figure 19: Profile, plan and section diagrams of Mulloon Creek over geologic time, showing a reduction of sinuosity and increasing incision and stream continuity after European settlement. PIA: post-incision alluvium (Johnston & Brierley 2006).

Colluvial sediments on the hillslopes that flank the valley, including those that form the piedmont in the west, are sourced proximally and have been transported directly from the adjacent hillslopes. As a consequence, these sediments are typically formed from a single rock type (monomict sediments). This differs from the alluvium on the floodplain, which is deposited as a result of fluvial activity, with sediments generally finer-grained and sourced more distally from the Mulloon Creek upper reaches and headwaters to the south. Consequently, the floodplain and alluvial terrace sediments are formed from a mixture of rock types (polymict sediments). The flood plain profile generally has more sand at depth and more clay closer to the surface (Johnston & Brierley 2006). This implies higher hydraulic flow conditions in order to deposit sand, followed later by lower flow conditions (flooding of flood plains) that could only carry and deposit clay-sized particles (Johnston & Brierley

2006). There are discontinuous gravel lenses in the alluvium that would have been former channels and sand bars from a time when the stream had a more braided form (Johnston & Brierley 2006). These gravel lenses have higher hydraulic conductivity than the surrounding alluvium, so may be the most likely vector for interaction between stream and shallow groundwaters. However, they may be more continuous sub-parallel to the contemporary stream and not persist laterally within the flood plain profile.

The area surrounding Mulloon Creek was heavily cleared when the first Europeans settled from 1820 (Johnston & Brierley 2006). Soils in this landscape, especially those developed over Ordovician metasediments and associated colluvium and alluvium, are typically sodic and are predisposed to erosion. Since the early 1800s the land has been used for crop agriculture and as grazing pasture for sheep and cattle, which has contributed to significant gully erosion and degradation of the landscape (Figure 19) (Jenkins et al. 2010a; Thackway 2019). Dry sclerophyll forests are now the predominant vegetation assemblage on both sides of Mulloon Creek (Jenkins et al. 2010b). The study site has been managed under the principles of NSF since 2006 (Hickson 2017). This has involved installing 27 leaky weirs in the immediate Mulloon Creek study site (Figure 18), as well as extensive revegetation of the riparian zone.

## 4. Methods

### 4.1 Fieldwork

Fieldwork was carried out in September 2020. Stream samples were collected from four locations up and downstream of the transects. Groundwater samples were collected from along two transects (T3 and T4) of existing piezometers that cut across the Mulloon Creek. The transects are subparallel with approximately 2.2 km between them. The southern, upstream transect (T3) consists of 13 bores. The northern, downstream transect (T4) has 13 bores. Comparison of samples from along each transect will give insight into water movement across the floodplain, while comparing sites between transects will show how water composition changes in the direction of streamflow.

Bores along T3 were installed in December 2016. These bores have 50 mm internal diameter PVC casings. At the bottom of each bore is a 100 mm unscreened sump to allow for clay deposition over time. The casings are screened from the top of the sump to within 1 m of the surface, with 1–2 mm screed sand. The T4 bores were installed in December 2019. These bores have 90 mm internal diameter PVC casings, 90 mm bottom sumps, and are screened from the top of the sump to varying heights, depending on the approximate heights of the aquifers at that point. The screened sections are encased by 1-2 mm screed sand. On top of the sand is a 30 mm bentonite plug, with spoil from bore drilling on top, up to 1 m from soil surface. Another bentonite plug is on top, until 400 mm from the soil

surface. The upper 400 mm is cemented. Some alluvial piezometer sites have two nested bores. At these sites, the shallow bore aims to hit a clay-rich layer; the deeper bore, a sand-rich layer.

Table 2: Field notes and ionic balances for ground and stream water samples from two transects at Mulloon Creek, NSW, September 2020. MCLRP: Mulloon Creek Landscape Rehydration Project.

	Sample ID	Notes	Ionic balance (%)
<b>Groundwater</b>	MCLRP38	Not filtered in field	19.3
	MCLRP39		-0.3
	MCLRP40	Not filtered in field	2.4
	MCLRP41-1		20.5
	MCLRP41-2	Could not purge	
	MCLRP42-1		10.9
	MCLRP42-2	Could not purge	
	MCLRP43		-2.9
	MCLRP44		7.9
	MCLRP45		-2.3
	MCLRP46		3.6
	MCLRP47	Not filtered in field	-2.6
	MCLRP48	Not filtered in field; RMIT anion results used	-7.4
	MCLRP49	Dry	
	MCLRP50	Not filtered in field	1.0
	MCLRP51		-0.5
	MCLRP52	Not filtered in field	1.1
	MCLRP53	Not filtered in field	6.1
	MCLRP54		-4.7
	MCLRP55	Not filtered in field	12.9
	MCLRP56		7.0
	MCLRP57	Not filtered in field	-4.5
	MCLRP58		-6.4
	MCLRP59	Not filtered in field	-3.2
	MCLRP60		-5.6
	MCLRP77		-3.0
	<b>Stream water</b>	PALERANG X-ING	
T3 LEAKY WEIR			-7.3
T4 LEAKY WEIR			-1.3
T4 LANEWAY			-6.1
<b>Duplicates</b>	DUP01	MCLRP39	-0.2
	DUP02	MCLRP45	-3.9
	DUP03	T4 LANEWAY	-6.5

Initial bore height and depth were measured with a tape. Three bore volumes were then purged from each piezometer, using an electric pump or manual bailing. Pumping allows new groundwater to enter the bore to be sampled, to prevent sampling of bore water that has been mixed with surface water. Pumped water was collected and used subsequently for

irrigation. During pumping, water quality parameters (water temperature, EC and pH) were measured periodically (Orion 5-Star multiparameter portable meter). After bore recharge, samples were collected and filtered with 0.45  $\mu\text{m}$  syringe filters, unless dissolved solid load made it infeasible to filter in the field. These samples were later filtered at RMIT. Samples were transferred to 100 mL HDPE bottles, labelled, and kept cool. Multiple bottles were filled for each sample to allow separate analysis of anions, cations and stable isotopes. For cations samples, water was acidified to pH of 2 so transition metals would be put into their most stable form. Samples that could not be filtered in the field were not acidified in the field. For samples that were laboratory-filtered, results for Ca and Mg may be overestimated, because adsorbed ions may have been released into solution between sampling and filtering. Also, Fe, Al and Mn in these samples may be underestimated due to ion precipitation.

Duplicate samples were collected at three sites (Table 2). Two bores did not recharge after pumping and one bore was dry, so samples were not collected for these sites. Alkalinity titrations were conducted in the field for some samples and in the lab for those samples that could not be filtered in the field. Field alkalinity measurement was conducted by titrating 10 mL of sample with 0.103 M HCl.

#### 4.2 Hydraulic potential

For each transect, the hydraulic gradient was calculated between a) each nested piezometer site and its neighbouring sites, b) the stream and the bores closest to the stream and c) the stream and the farthest bore sites from the stream. The DEM elevation data being used have not been hydro-flattened, which would give greater accuracy of stream elevation (Toscano et al. 2015). In addition, the LIDAR data collection occurred seven years prior to the present sampling work, meaning the stream grade may have been different at the time of sampling.

Surface elevation and stream grade data were attained from LIDAR digital elevation models (DEMs) (NSW Government Spatial Services 2015). Vertical spatial resolution is 1 m with accuracy of  $\pm 0.3$  m (95% CI), so results that show aquifer and land elevation differences  $< 0.3$  m are ignored in the analysis. Cross section diagrams illustrate surface elevation, water table head and stream grade along each transect. Hydraulic gradients give insight into the direction of water movement along transects. However, lacking a network of piezometers, it is only possible to analyse gradients along a single plane (perpendicular to stream flow). Sample EC is plotted on the cross-section diagrams to visualise the extent of mixing in the hyporheic zone and floodplain.



### 4.3 Laboratory analysis

#### **Isotope analysis**

Stable water isotopes ( $\delta^{18}\text{O}$  and  $\delta^2\text{H}$ ) were measured at Australian National University (ANU) (Picarro L2140i Cavity Ring-Down Spectrometer). One sample (piezometer 48) was misplaced and was therefore not analysed. Values of  $\delta^{18}\text{O}$  and  $\delta^2\text{H}$  were categorised by location and plotted against each other to analyse evaporation trends. Local meteoric water lines for Braidwood and Bungendore were included on the chart to ascertain the likely origin of water from the sample sites. The LMWLs were constructed by Gray et al. (2018) using a precipitation weighted reduced major axis regression (PWRMAR) developed by Crawford et al. (2014). Deuterium excess values were calculated and plotted on a map image to visually represent spatial distribution.

#### **Hydrogeochemistry**

Anions ( $\text{F}^-$ ,  $\text{Cl}^-$ ,  $\text{Br}^-$ ,  $\text{NO}_3^-$ ,  $\text{SO}_4^{2-}$ ) were measured at ANU (Thermo Fisher Dionex Ion Chromatography). Anions were also measured at RMIT (Thermo Fisher Dionex ICS 1600). ANU anion results were used for all data analysis, except for one sample that was not analysed at ANU. For this sample, the RMIT result was used (Table 2). Major cations ( $\text{Na}^+$ ,  $\text{Mg}^{2+}$ ,  $\text{Ca}^{2+}$ ,  $\text{K}^+$ ) were measured at RMIT (Agilent Technologies 4200 MP-AES). Minor cations and trace elements (Be, Al, K, V, Cr, Mn, Fe, Co, Ni, Cu, Zn, As, Se, Mo, Ag, Cd, Ba, Tl, Pb, Th, U) were measured at RMIT (Agilent 7700 ICP-MS with Micro Mist nebuliser and ASX-500 autosampler). Laboratory alkalinity titrations for samples not titrated in the field were conducted at RMIT. Samples were filtered with 0.45  $\mu\text{m}$  syringe filters. Four drops of phenolphthalein indicator were added to 50 mL of each filtered sample and titrated against 0.005 M HCl until colour change to determine total alkalinity.

Chemical analysis at RMIT used volumetric determinations and analysis at ANU used gravimetric determinations. In data analysis, a density of is 1 g/mL for all water samples is assumed. A charge balance was conducted using all major ion data and minor cation data. Absolute charge imbalance was calculated as < 10% in 27/30 samples, including duplicates (Table 2). One sample had an imbalance of 10.9%, one sample 12.9% and two samples > 20%. All samples are still included in the analysis, as they are indicative of a qualitative relationship, but should not be assumed to be quantitatively exact.

A Piper diagram is used to classify water samples according to their geochemical molar concentrations (Cook & Herczeg 2012). The plot is made up of one trilinear diagram for anions and one for cations. The relative molar concentrations of each major ion are plotted along each axis. These two trilinear plots are then combined in a diamond plot above. The TDS measurement of each sample is visualized by the sizes of the circles in the diamond plot. The Piper plot allows initial classification and analysis of water, but it is not sufficient to uncover underlying geochemical processes.

## 5. Results & Discussion

### 5.1 Hydraulic potential and electrical conductivity

#### Transect 3

On T3, all 12 gradient measurements are  $< 0.06$ . The largest gradient (0.05) is between the stream and the shallow Ordovician metasediment hillside bore on the furthest western edge of the transect. Four sites had aquifer elevation differences less than the DEM vertical accuracy of 0.3 m. These were recorded as having zero gradient.

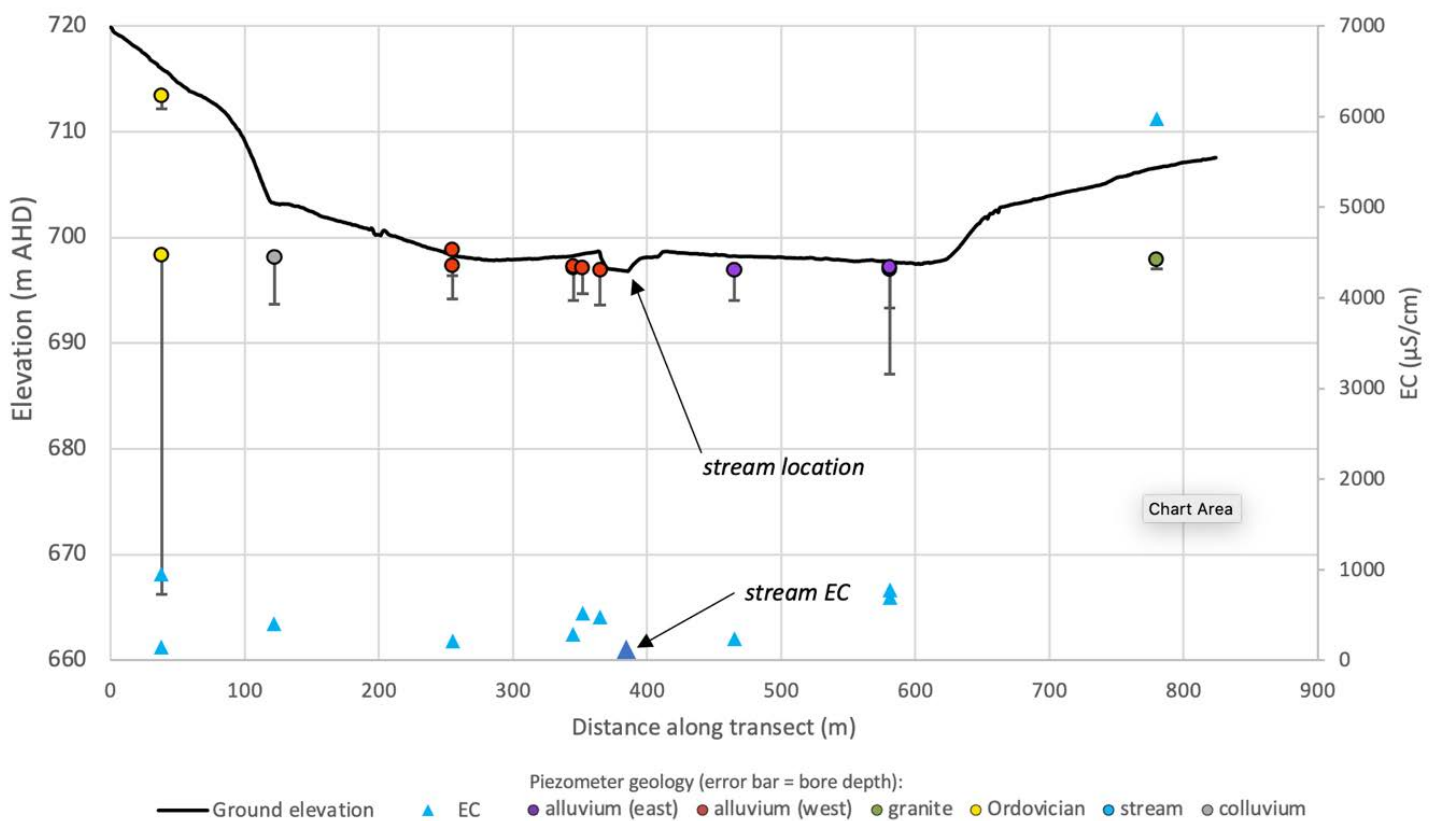


Figure 20: Transect 3 piezometer depth, hydraulic potential and EC, and stream water level and EC. Mulloon Creek, NSW, September 2020.

Along T3, the direction of hydraulic gradients implies the stream should be gaining. However, the low absolute head implies any mixing is occurring at a slow pace. These data do not support the assertion that the leaky weirs create conditions for a losing stream. It is possible that leaky weirs temporarily hold back groundwater from entering the stream, thereby keeping more groundwater in shallow aquifers. However, in dry times when there is less or no upstream flow, the groundwater may enter the channel. This would contradict the NSF assertion that weirs can keep the landscape hydrated in droughts.

### Transect 4

On T4, the range of gradients was 0 – 0.04. The bores on both ends of T4 have lower potential than the stream head. However, all other bore sites on the transect sit higher than the stream, indicating that the stream is gaining, if there is any mixing happening. Bore 77 is a deep bore that taps Ordovician metasediment below the alluvium. The high potential in the piezometer here implies there could be deep groundwater pushing upward into the alluvium, mixing with shallow Ordovician groundwater from upslope and also any stream water that has entered the alluvium. The western slopes are higher elevation than those on the east, meaning there is more potential for groundwater to be stored here, and for more mixing with Mulloon Creek to occur with water from this side compared to the east.

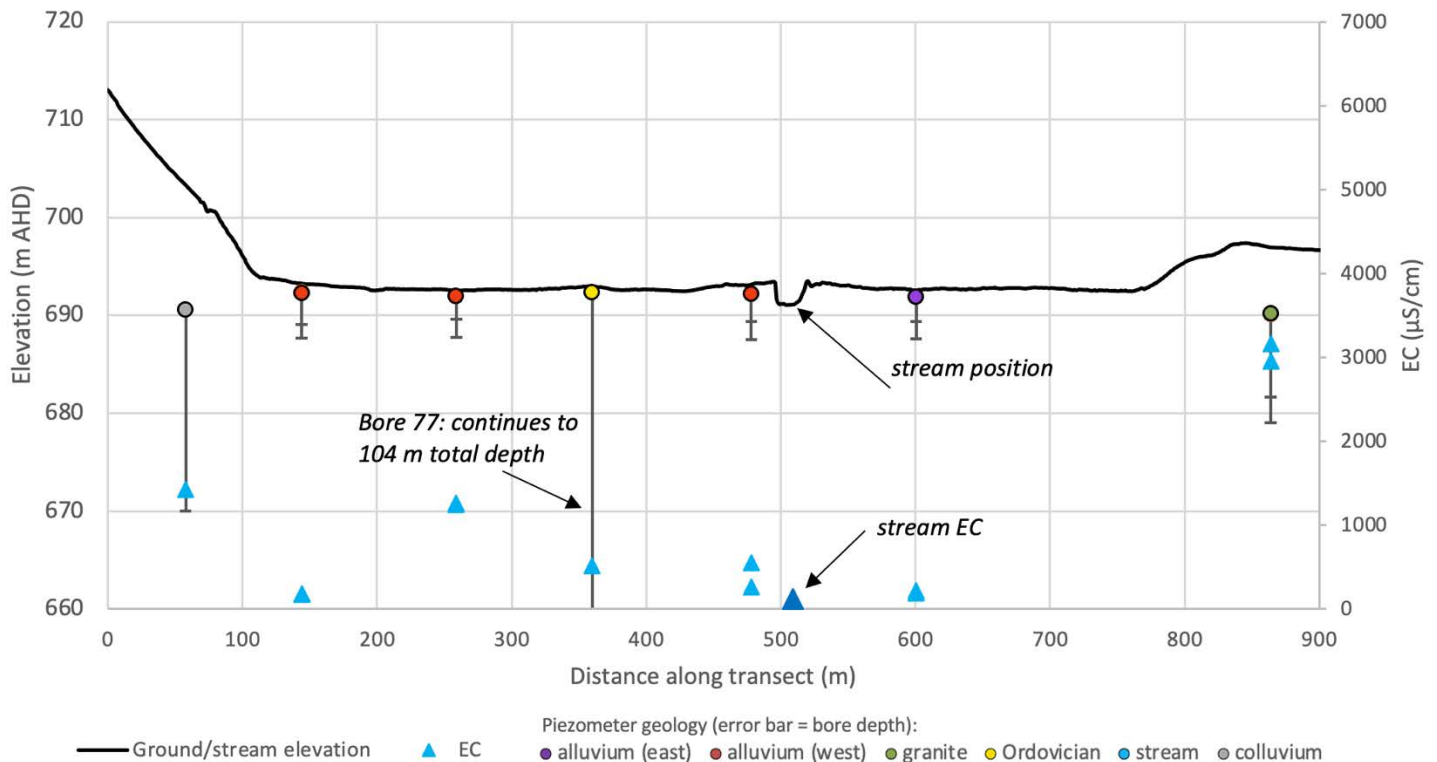


Figure 21: Transect 4 piezometer depth, hydraulic potential and EC, and stream water level and EC. Mulloon Creek, NSW, September 2020.

Along both transects, groundwater EC is lowest and most similar to creek EC at sites closest to the stream. Groundwater EC then increases rapidly on the eastern bank and less rapidly travelling west from the stream. These data imply there is mixing in the hyporheic zone. However, there is no evidence that the weirs are causing or increasing this mixing. At bore sites further from the stream, it is possible the groundwater becomes more influenced by deeper basement water that rises and mixes with more recent additions from the stream. Though, floodplain muds may impede this vertical movement.

## 5.2 Stable isotopes

Groundwater  $\delta^{18}\text{O}$  is between -8.68 – -5.31 ‰ VSMOW; stream water is between -7.36 – -6.93 ‰ VSMOW (Table 3). Groundwater  $\delta^2\text{H}$  is -55.19 – -30.87; stream water: -41.48 – -39.83 ‰ VSMOW. Deuterium excess (D-excess) in groundwater is 11.6 – 17.28, and 15.56 – 17.36 in stream samples.

Table 3: Water stable isotope data for groundwater and stream sites at Lower Mulloon, September 2020.

Transect/stream	Sample ID	$\delta^{18}\text{O}$ (‰ VSMOW)	$\delta^2\text{H}$ (‰ VSMOW)	Deuterium excess
T3	MCLRP38	-8.90	-53.90	17.28
T3	MCLRP39	-7.81	-45.96	16.49
T3	MCLRP40	-7.73	-44.53	17.27
T3	MCLRP41-1	-7.61	-45.19	15.67
T3	MCLRP42-1	-5.31	-30.87	11.60
T3	MCLRP43	-6.24	-37.96	11.86
T3	MCLRP44	-6.34	-37.14	13.58
T3	MCLRP45	-5.54	-32.43	11.84
T3	MCLRP46	-7.71	-45.87	15.87
T3	MCLRP47	-7.34	-44.78	13.97
T3	MCLRP48		not measured	
T4	MCLRP50	-8.05	-48.26	16.21
T4	MCLRP51	-8.63	-52.84	16.26
T4	MCLRP52	-8.50	-51.08	16.90
T4	MCLRP53	-8.05	-48.18	16.24
T4	MCLRP54	-7.91	-46.58	16.78
T4	MCLRP55	-5.56	-32.41	12.17
T4	MCLRP56	-6.60	-37.13	15.61
T4	MCLRP57	-8.68	-55.19	14.22
T4	MCLRP58	-5.97	-36.08	11.72
T4	MCLRP59	-6.94	-42.71	12.78
T4	MCLRP60	-6.15	-37.32	11.88
T4	MCLRP77	-8.37	-50.08	16.91
Stream	Palerang Crossing	-7.36	-41.48	17.36
Stream	T3 Leaky Weir	-7.23	-41.17	16.85
Stream	T3 Leaky Weir	-7.16	-40.99	16.32
Stream	T4 Laneway North	-6.93	-39.83	15.56

All stream and most groundwater samples plot close to the Braidwood LMWL (Figure 22). This implies the waters are locally recharged and originate from rain falling in the area around Braidwood. This is despite the fact the study site is closer to Bungendore than Braidwood. At most groundwater sample locations, stable isotope composition is less enriched than the surface water, meaning the surface water has undergone more evaporation than the groundwater. There is also no obvious mixing trend, where intermediary alluvial waters would sit between groundwater and stream water end

members. This implies the water in the floodplain aquifers does not originate from the stream. Rather, it is more likely the water in the shallow aquifers has risen from deeper Ordovician basement groundwater.

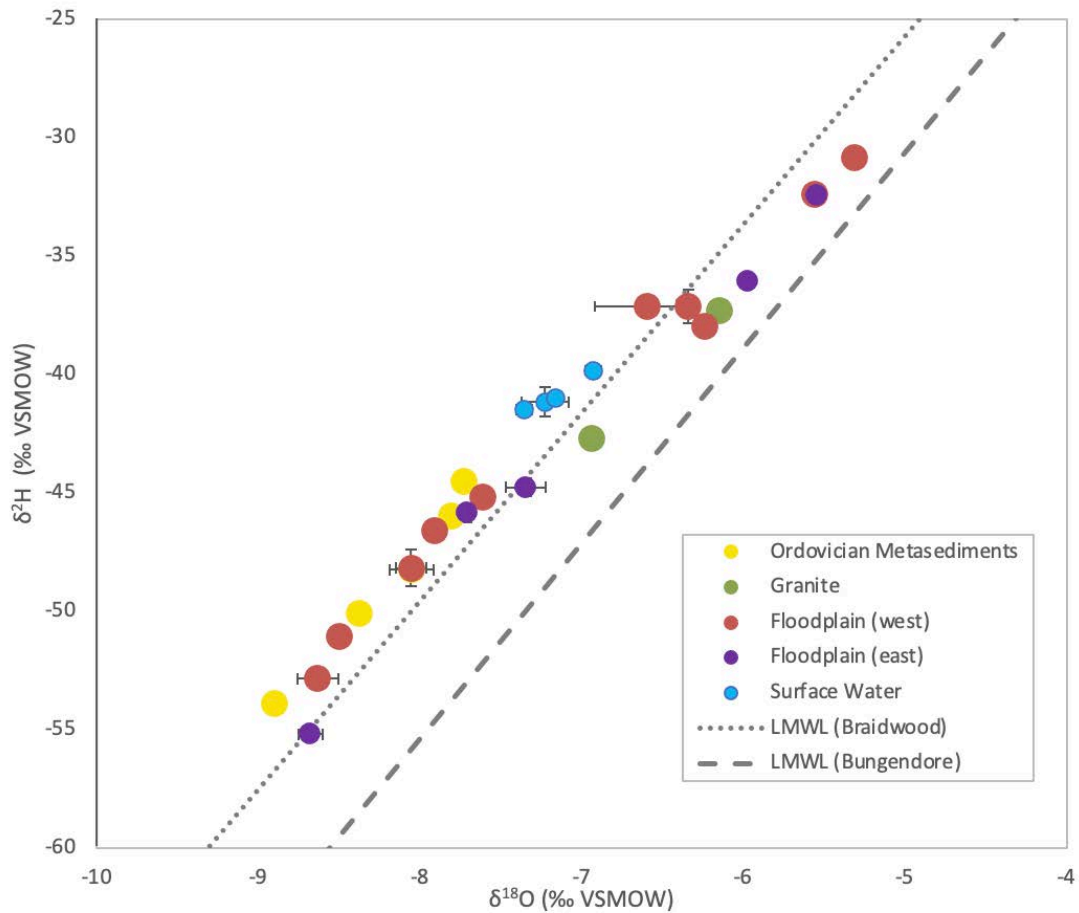


Figure 22: Stable water isotope composition of stream and groundwaters at Lower Mulloon, September 2020. Error bars represent standard deviation (some SD values are too small to be visible on the plot). LMWLs from Gray et al. (2018).

D-excess values are highest further away from the Creek, lower at the creek edge and increases again in the stream samples (Figure 23). The difference between the D-excess of stream and near-stream samples implies that, at the time of sampling, there was not significant mixing occurring. The sample from the deep Ordovician bore (Site 77) has similar isotope values to the nearby shallow aquifer. This implies both locations have been recharged by local rainfall in a recent period, perhaps 5 – 10 years. On the western side, stable isotope and hydraulic head data imply water is being pushed downslope from the western hills into the floodplain.

The groundwater samples from the eastern, granite side of the Creek have lower D-excess values than the western side, implying there is a greater propensity for evaporation from the regolith on this side. Stream D-excess is progressively lower in samples that are further downstream, which is predictable, as water will evaporate as it travels.

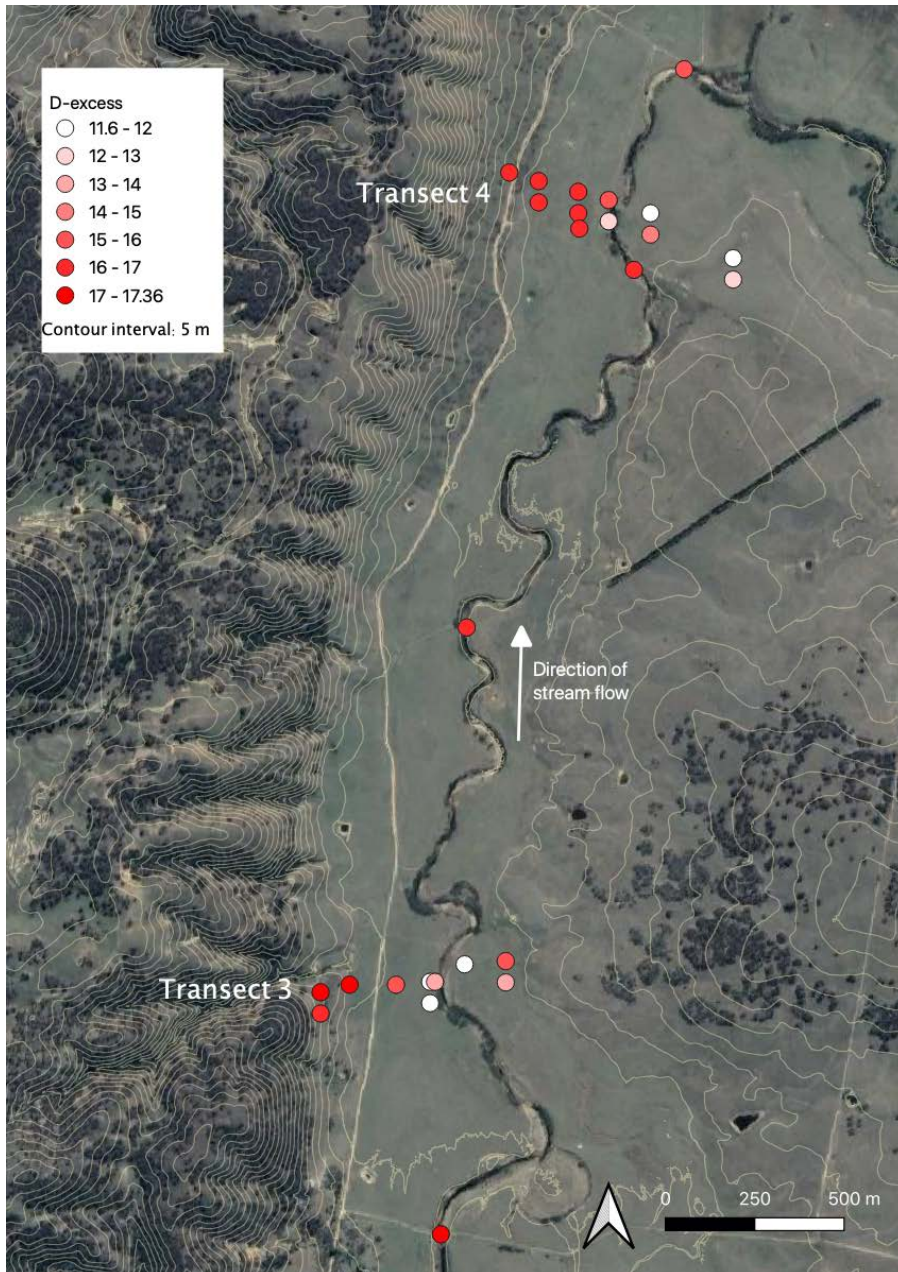


Figure 23: Deuterium excess values for ground- and stream water samples at Lower Mulloon, September 2020.

Data capture was limited to a single sampling event. Stable isotope composition may vary throughout the year, so these data may not be representative of the actual connection between stream and groundwater. A quarterly sampling schedule over at least two years would capture seasonal fluxes and provide more robust data.

### 5.3 Geochemistry

Total dissolved solids (TDS) concentrations for groundwater samples ranged from 91 – 3456 mg/L (Appendix 1). Stream sample TDS was between 78 – 80 mg/L. Groundwater on the eastern granite banks had the highest dissolved salt load, and stream samples the lowest (Figure 24).



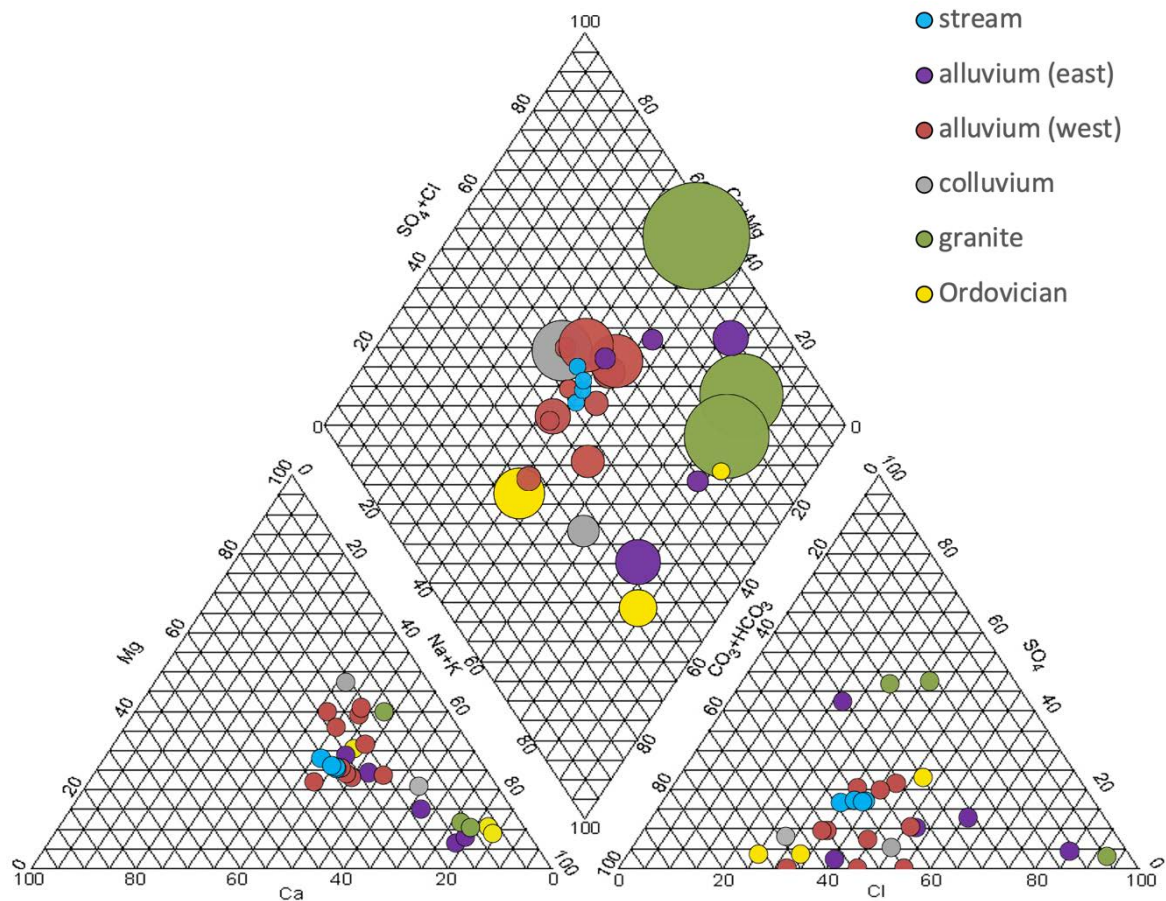


Figure 24: Piper diagram characterising dissolved ions in stream and groundwater samples along Mulloon Creek, September 2020. Circle sizes in the diamond plot correspond to sample TDS.

For cations, samples are broken into two groupings: the stream and some surrounding groundwater are mixed type, while a grouping of western alluvial, Ordovician and granite sites are strongly dominated by Na (Figure 24). Plotted spatially, these groups reveal a contiguous band of Na+K type sites in the east on T4, and isolated Na+K sites on T3 (Figure 25). For the anion segment of the Piper plot, all stream and most alluvial samples are of mixed type, while most Ordovician and some alluvial sites are HCO<sub>3</sub> type. The remaining sites, mainly in the east, are Cl type. Ordovician sites comprise sulfide-bearing marine deposits, including disseminated pyrite, which oxidises during weathering and releases SO<sub>4</sub> salts. This leads to a slightly elevated SO<sub>4</sub> signature for these samples. Ordovician groundwaters would be expected to be higher in SO<sub>4</sub> relative to granite groundwaters, as the granitic geology does not contain sulfidic minerals. This is the case along T3. But on T4, granite groundwater samples have high SO<sub>4</sub> (Figure 27). This could be a result of sulfur gas exchange between the soil and the atmosphere, although there is limited evidence for this process. It also is more likely to originate from clay and organic material transported by land managers from elsewhere to mix with the existing sand. Alternatively, it may have originated from alluvial material from upstream Ordovician metasediment sites.

In addition to being high in  $\text{SO}_4$ , the granite groundwater on T4 is NaCl fluid. Granite aquifers normally have relatively fresh water running from them because the base minerals do not easily weather (Cook & Herczeg 2012). The high salt signal in these samples is from salt accumulation and storage and possibly some evaporative concentration near surface, not primary weathering. During granite weathering K-feldspar (orthoclase) and Na plagioclase feldspar (albite) weather through smectite to kaolinite ( $\text{Al}_2\text{Si}_2\text{O}_5(\text{OH})_4$ ). Quartz ( $\text{SiO}_2$ ) is present, but it is chemically inert and will not generally contribute ions to groundwater. Minor mafic minerals include biotite and hornblende. Biotite weathers to vermiculite and hornblende, through Fe-smectite to kaolinite, with the weathering of both minerals releasing small amounts of Fe, Mg and Ca ions. Typically, the Ca is lost in solution, but the Fe and Mg may be incorporated into secondary oxides (e.g., haematite) and oxyhydroxides (e.g., goethite).

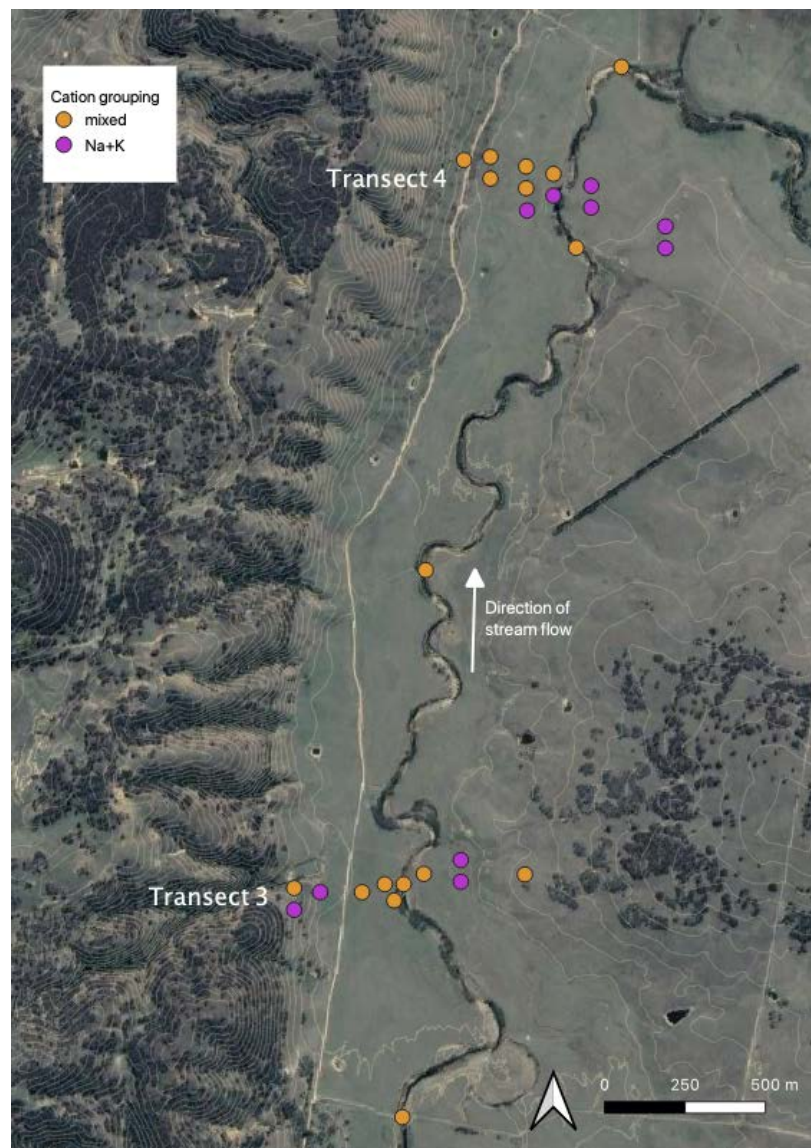


Figure 25: Cation groupings for stream and groundwater sample sites at Lower Mulloon, NSW, September 2020.



On the combined plot in the Piper diagram, most samples are of mixed type, plotting near the centre of the diamond. Most eastern sites and one Ordovician site on the west were Na-Cl type, and three western alluvial and one Ordovician site were Mg-HCO<sub>3</sub> type. The western alluvial sites have the most overall chemical similarity to the stream samples, mixed HCO<sub>3</sub> and Cl type. Where the regolith veneer is relatively thin, for example over the Ordovician metasediment rocks at Mulloon, there is less salt accession and storage. Shallow groundwater may have HCO<sub>3</sub> as the dominant anion because infiltrating rainwater interacts with CO<sub>2</sub> in soil pores, forming carbonic acid and HCO<sub>3</sub>. Water emerging from areas where there is stored Cl in the regolith can combine with HCO<sub>3</sub>-bearing water to give the mixed type waters. As distance from the stream increases, the chemical composition of groundwater diverges from the stream chemistry. This implies there may be a connection between the stream and the proximal alluvial plain, particularly on the western side. However, these data are not sufficient to conclude that a) the direction of water movement is from the stream into the floodplain aquifer nor b) the leaky weirs are causing this connection. If there is stream-aquifer connectivity, it may be the result of water flux from alluvium into the stream.

### **Chloride ratio plots**

If we compare Transect 3 and Transect 4, corresponding locations on each transect tend to have similar chemical signatures, implying that similar hydrogeological processes are occurring in each given substrate environment. K-feldspar (orthoclase) and minor K-bearing mica (muscovite) reacts with dilute acids (water, carbonic acid), releasing K ions into solution as they weather to kaolinite and illite respectively. This may be the origin of the elevated K values at some alluvial sites (Figure 26 and Figure 28). Three western alluvial sites have high ratios of Zn/Cl, K/Cl and HCO<sub>3</sub>/Cl (Figure 27), which may be a result of fertiliser application in these areas.

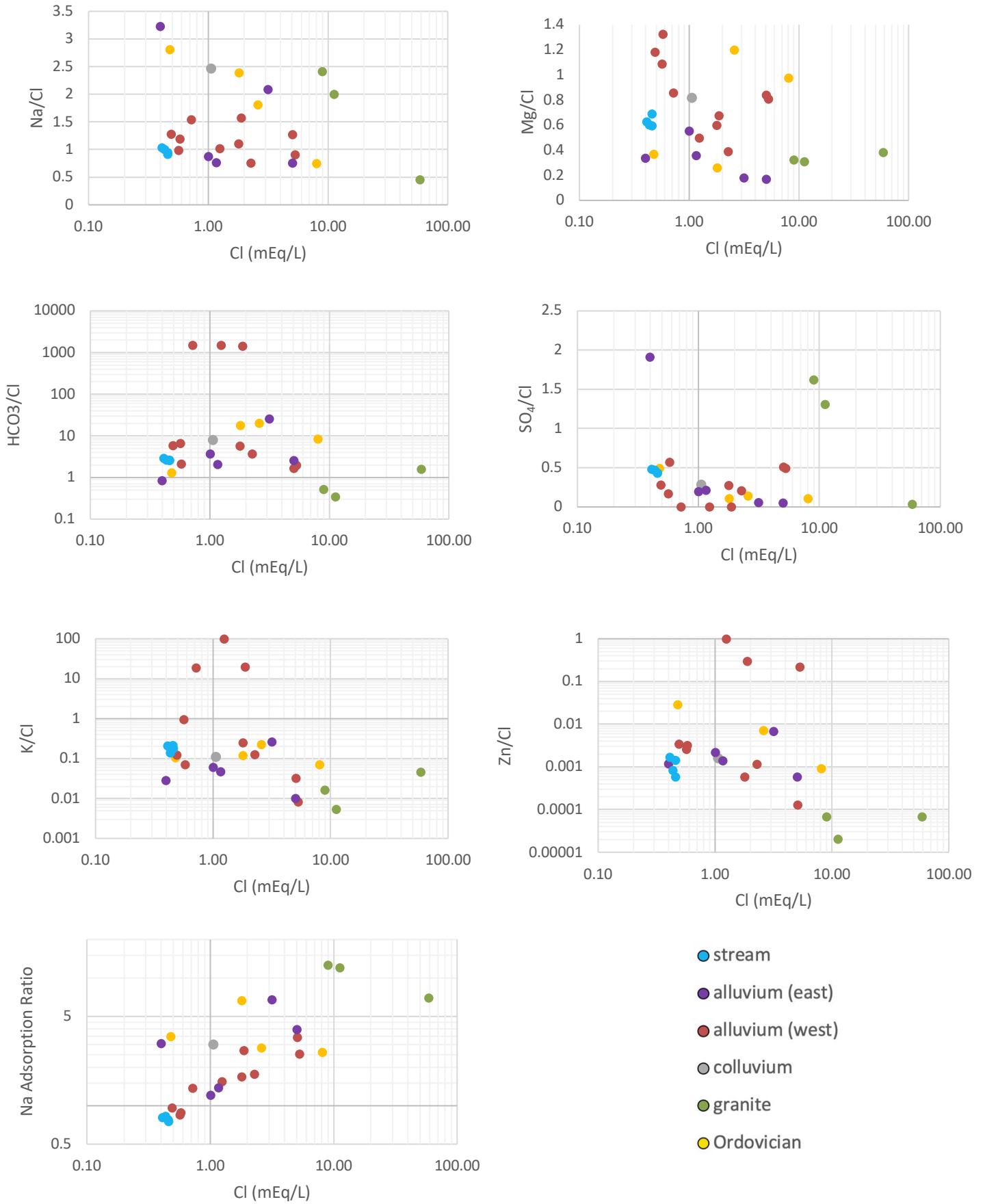


Figure 26: Ion ratios plotted against Cl values for surface and groundwater samples collected at Lower Mulloon, September 2020.

The western alluvium has similar Na/Cl values as the stream (Figure 26), however, some sites have more Na suggesting the stream is not the source of the Na in the groundwater. Mobilisation of salt via cation exchange in the alluvium may be the source of this additional Na. Also, the clay-rich Ordovician metasediments may concentrate salts after high rates of evaporation. Some Ordovician groundwater samples have high Mg/Cl values (Figure 26 and Figure 27). This may be the result of reverse ion exchange, which occurs when Na enters the system and dislodges Ca and Mg from clay particles.

This is further evidenced by the Sodium Adsorption Ratio (SAR) values for some Ordovician sites (Figure 26). In cases where Na-rich water is continually added to a system, Na is adsorbed onto clay particles, and soil will become friable and crumbly, and potentially more dispersive and sensitive to erosion. Leaky weirs create additional hydraulic pressure in areas with sensitive sodic soils. This may result in gully erosion occurring around the side of a semi-rigid weir. As such, land managers should understand the importance of revegetating riverbanks near leaky weirs and monitoring for signs of sediment mobilisation. These results agree with Hickson's (2017) findings that Mulloon sodic soils may be vulnerable to erosion near leaky weirs.

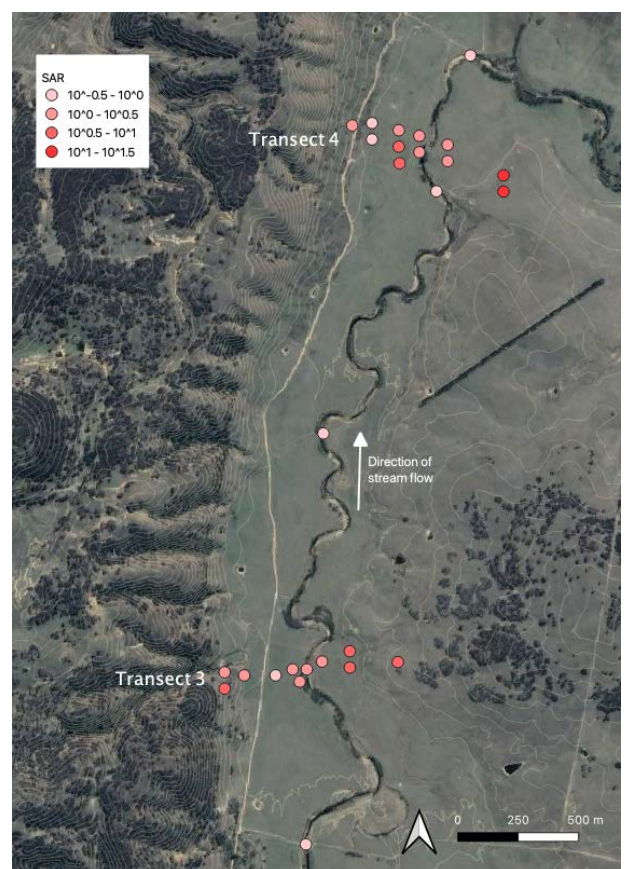
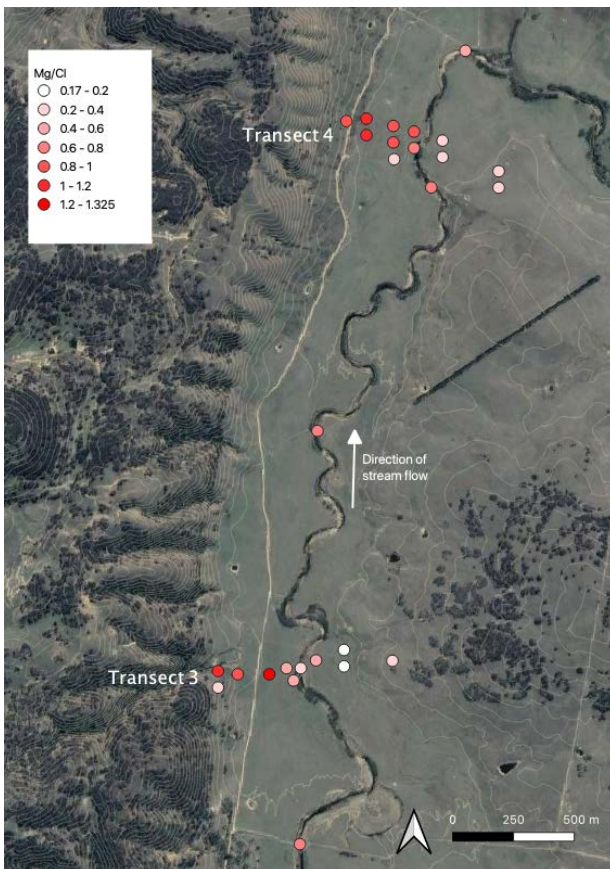
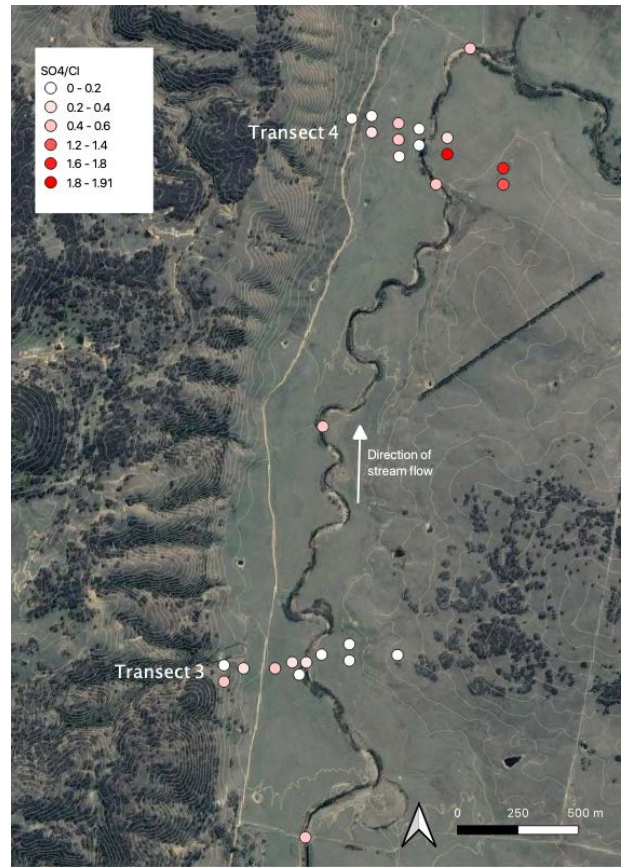
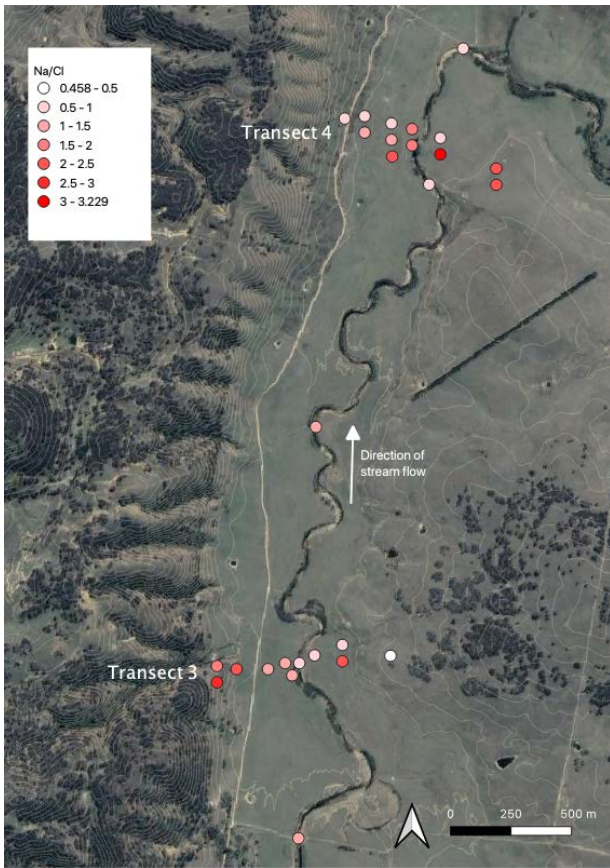


Figure 27: Maps of Lower Mulloon sample sites, showing Cl ion ratio values for Na, SO<sub>4</sub>, Mg and SAR.



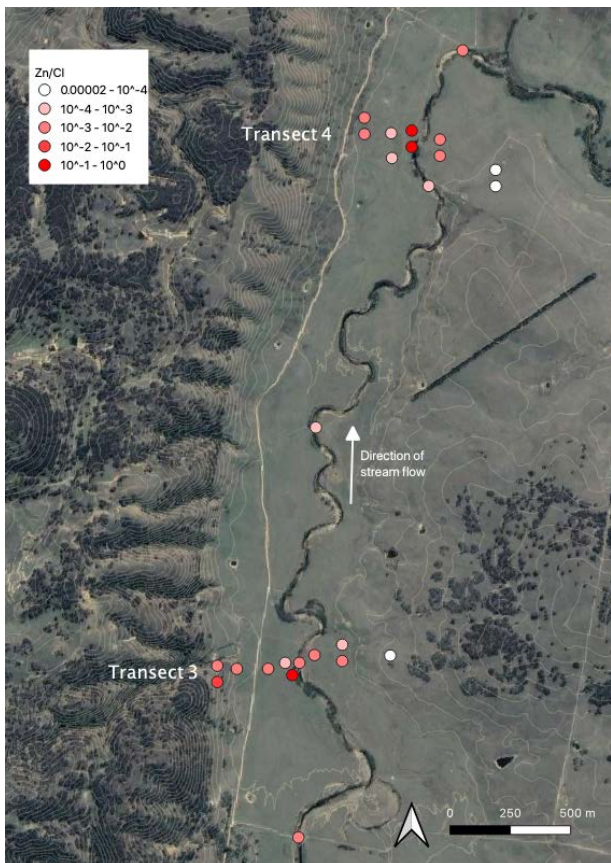
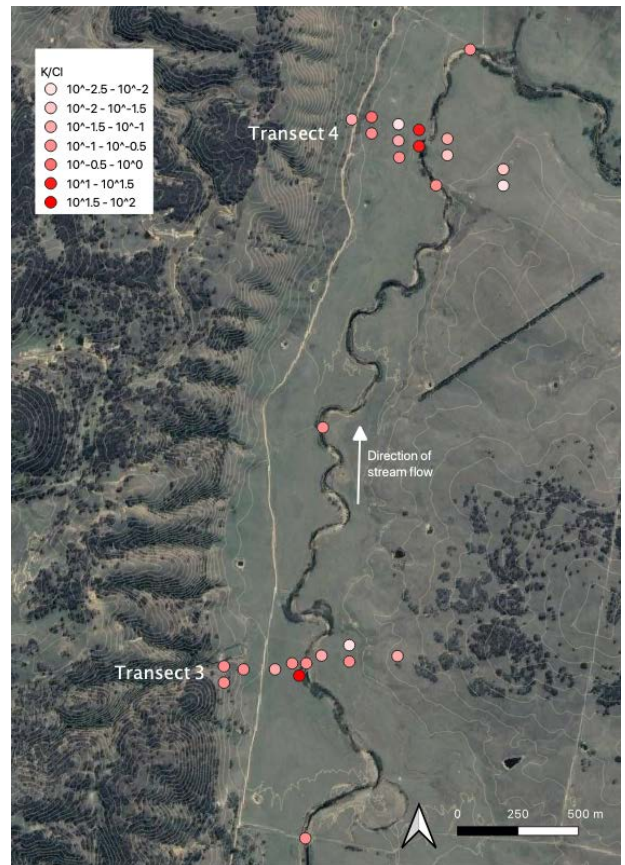
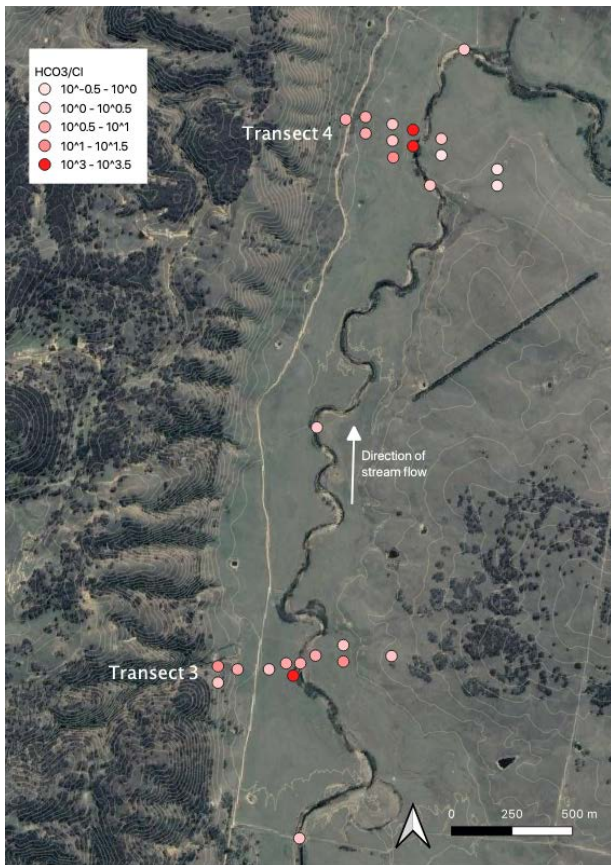


Figure 28: Maps of Lower Mulloon sample sites, showing Cl ion ratio values for HCO<sub>3</sub>, K and Zn.

## Discussion

The model for salt accession over an extended timeframe in this area is dominated by aeolian input from the west and an oceanic flux in rainwater from the east, with localised contribution from rock weathering (Moore et al. 2018). The groundwater on Ordovician geology is expected to be more saline than waters at granite sites because elsewhere in this landscape the Ordovician metasediments with thicker regolith veneer store and release salt readily (Moore et al. 2018). But at this site, the Ordovician side is high relief, with a relatively thin regolith veneer. In this part of the landscape there is also elevated hydraulic head influencing groundwater. Relative to the Ordovician fractured rock, colluvial slopes and proximal alluvial landscape in the west, the granitic landscape in the east has a thicker regolith veneer and hence a greater capacity naturally store salt. The result is less salt storage on the west compared to the east. On the Ordovician range the soils are skeletal, and the colluvial sediments are clast-supported, limiting capacity for salt storage, and enhancing water movement downslope. On the granite, a relatively thick regolith veneer equates to greater capacity to store salts naturally deposited in the landscape. Salt stored in the regolith is mobilised when water moves through the landscape, causing an elevated salinity signature in the east.

These geochemical results are consistent with prior analysis of comparable ground and surface waters atop Ordovician and granite geologies in the Upper Murrumbidgee catchment (Gray et al. 2019). The data also align with the findings of Keene et al. (2007), who found evidence for leaky weirs enhancing localised mixing in the hyporheic zone close to the weirs.

The geochemical and isotope data imply that there is a contribution from Ordovician basement groundwater and surface water in the shallow alluvial aquifer. The working model is that the in-stream leaky weirs are enhancing lateral stream water movement into the flood plain and alluvial terraces. However, significant hydraulic potential due to lateral and upward movement of groundwater may be holding back the Creek water, preventing it from spreading extensively into the adjacent floodplain. It follows that the leaky weirs do not force stream water to enter alluvium. Rather, the weirs prevent groundwater from entering the stream as fast as it otherwise might. This would mean land managers would see variations in floodplain hydration related to year-on-year changes in rainfall. In this case, the leaky weirs would not provide deep resilience and reliable water in times of drought, apart from in the riparian zone.

The muddy floodplain has low permeability, which may inhibit recharge of floodplain aquifers by the stream. Lenses of more permeable gravel are present, remnants of high stream-flow event transport and lateral stream migration. However, lenses may be more continuous along the valley, sub-parallel to the stream. The lenses are commonly not laterally continuous into the floodplain, and so are not likely to be a vector of significant

rehydration. Similar results were reported in a prior study of Mulloon Creek, which found that clay-dominant sites will reduce the impact of mixing near weirs and that sodic soils at weir locations may lead to harmful dispersion (Hickson 2017).

Overall, these geochemical data present the possibility of mixing between stream and proximate shallow groundwaters. The water stable isotope data implies that there is limited localised mixing. More data is required over an extended period to enable more detailed quantification of the true impact of the leaky weirs on the rehydration of the floodplain by stream water. In particular, seasonal measurement of water stable isotope data would allow for a much more accurate model of water movement through the landscape under different conditions and over longer time periods. Mass balance calculations for both ion geochemistry and isotopes can then be completed. This geochemical modelling would help build a picture of the relative contributions of interflow, deep groundwater and stream water in the shallow aquifers.

## 6. Conclusions

Hydrometric, isotopic and physicochemical data were used to assess water and salt movement in the Mulloon Creek floodplain. The hydraulic gradient data imply limited flux of water between Mulloon Creek and its surrounding shallow aquifers at the sample sites. This conclusion is supported by the water stable isotope data, which show there are different sources for stream and groundwater recharge. There is also evidence that shallow aquifers are partially recharged from lateral flow and upwelling of deeper groundwater.

Water geochemistry results present the possibility that there is linkage between stream and near-stream aquifers, particularly on the western side of the creek. However, the direction of flow may not be from stream to groundwater. So, it is not possible to say that the leaky weirs are forcing stream water to travel laterally into the aquifer. To build a more accurate model of water movement caused by leaky weirs, repeated sampling must be undertaken over a longer period. This would capture seasonal variability in stream flow conditions.

It is important for NSF managers to consider the possibility of lateral flow and deep upwelling of groundwater feeding shallow aquifers. It is also necessary to consider the soil types and regolith surrounding the location of prospective leaky weirs. If sodic soils are put under increased hydraulic pressure from leaky weirs, they may erode. As such, revegetation of riparian zones, along with consistent monitoring, must accompany weir construction in such settings.

## 7. References

- Andrews, P 2006, *Back from the brink: How australia's landscape can be saved*, ABC Books.
- Banks, EW, Simmons, CT, Love, AJ & Shand, P 2011, 'Assessing spatial and temporal connectivity between surface water and groundwater in a regional catchment: Implications for regional scale water quantity and quality', *Journal of Hydrology*, vol. 404, no. 1, pp. 30-49.
- Berner, EK & Berner, RA 1987, *The global water cycle: Geochemistry and environment*, Prentice-Hall, Eaglewood Cliffs, New Jersey.
- Bridge, JS 2003, *Rivers and floodplains: Forms, processes, and sedimentary record*, Blackwell, Oxford, UK.
- Brierley, GJ, Cohen, T, Fryirs, K & Brooks, A 1999, 'Post-european changes to the fluvial geomorphology of bega catchment, Australia: Implications for river ecology', *Freshwater Biology*, vol. 41, no. 4, pp. 839-848.
- Brierley, GJ & Fryirs, K 1999, 'Tributary–trunk stream relations in a cut-and-fill landscape: A case study from wolumla catchment, New South Wales, Australia', *Geomorphology*, vol. 28, no. 1-2, pp. 61-73.
- Brodie, R, Sundaram, B, Tottenham, R, Hostetler, S & Ransley, T 2007, *An overview of tools for assessing groundwater-surface water connectivity*, Bureau of Rural Sciences, Canberra.
- Bureau of Meteorology 2021a, *Monthly rainfall – Braidwood racecourse*, viewed 14/4/21, <<http://www.bom.gov.au/climate/data/>>.
- Bureau of Meteorology 2021b, *Monthly rainfall – bungendore post office* viewed 14/4/21, <<http://www.bom.gov.au/climate/data/>>.
- Cartwright, I & Morgenstern, U 2016, 'Using tritium to document the mean transit time and sources of water contributing to a chain-of-ponds river system: Implications for resource protection', *Applied Geochemistry*, vol. 75, pp. 9-19.
- Colquhoun, GP, Hughes, KS, Deyssing, L, Ballard, JC, Folkes, CB, Phillips, G, Troedson, AL & Fitzherbert, JA 2020, *New South Wales seamless geology dataset*, version 2, [Digital Dataset], Geological Survey of New South Wales, Department of Regional NSW, Maitland.
- Cook, PG & Herczeg, AL 2012, *Environmental tracers in subsurface hydrology*, Springer, Boston, MA.
- Crawford, J, Hughes, CE & Lykoudis, S 2014, 'Alternative least squares methods for determining the meteoric water line, demonstrated using gnip data', *Journal of Hydrology*, vol. 519, pp. 2331-2340.



Department of Planning, Industry and Environment 2021, *Australian soil classification (asc) soil type map of NSW, version 4.5*, Department of Planning, Industry and Environment, Parramatta.

Dobes, L, Weber, N, Bennett, J & Ogilvy, S 2013, 'Stream-bed and flood-plain rehabilitation at Mulloon creek, Australia: A financial and economic perspective', *The Rangeland Journal*, vol. 35, no. 3, pp. 339-348.

Environment Australia 1997, *The wetlands policy of the commonwealth government of Australia*, Commonwealth of Australia, Canberra.

Evans, JP, Argueso, D, Olson, R & Di Luca, A 2017, 'Bias-corrected regional climate projections of extreme rainfall in south-east Australia', *Theoretical and Applied Climatology*, vol. 130, no. 3, pp. 1085-1098.

Fanning, PC 1999, 'Recent landscape history in arid western New South Wales, Australia: A model for regional change', *Geomorphology*, vol. 29, no. 3, pp. 191-209.

Filkov, AI, Ngo, T, Matthews, S, Telfer, S & Penman, TD 2020, 'Impact of australia's catastrophic 2019/20 bushfire season on communities and environment. Retrospective analysis and current trends', *Journal of Safety Science and Resilience*, vol. 1, no. 1, pp. 44-56.

Fitts, CR 2013, *Groundwater science*, 2nd edn, Academic, Oxford.

Fitzherbert, JA, Thomas, OD, Deyssing, L, Bewert-Vassallo, KE, Simpson, CJ & Sherwin, L 2017, *Braidwood 1:100 000 geological sheet 8827*, Geological Survey of New South Wales, Maitland, <<https://search.geoscience.nsw.gov.au/product/50>>.

Fryirs, KA & Brierley, GJ 2013, *Geomorphic analysis of river systems: An approach to reading the landscape*, 1st edn, Blackwell Publishing Ltd.

Goldman, A, Graham, E, Crump, A, Kennedy, D, Romero, E, Anderson, C, Dana, K, Resch, C, Fredrickson, J & Stegen, J 2017, 'Biogeochemical cycling at the aquatic–terrestrial interface is linked to parafluvial hyporheic zone inundation history', *Biogeosciences*, vol. 14, pp. 4229-4241.

Gray, DR & Foster, DA 2004, 'Tectonic evolution of the lachlan orogen, southeast Australia: Historical review, data synthesis and modern perspectives', *Australian Journal of Earth Sciences*, vol. 51, no. 6, pp. 773-817.

Gray, S, McPhail, B, Hughes, C, Opdyke, B & Moore, L 2018, 'Interactions between meteoric, surface, and ground water in fractured rock: Upper Murrumbidgee catchment – preliminary results from meteoric and surface water studies', *XXII Meeting of the International Mineralogical Association: Book of Abstracts*, Melbourne, 13-17 August, Geological Society of Australia Inc., Sydney, p. 39.

Gray, S, Moore, L, Opdyke, B & Hughes, C 2019, *Identifying groundwater-surface water interactions and groundwater geochemistry in the upper Murrumbidgee catchment using surface water surveys*, Australasian Groundwater Conference: Groundwater in a Changing World, Flinders University, Brisbane, 24-27 Nov., [Poster].

Hazell, D, Osborne, W & Lindenmayer, D 2003, 'Impact of post-european stream change on frog habitat: Southeastern Australia', *Biodiversity & Conservation*, vol. 12, no. 2, pp. 301-320.

Healy, RW 2010, *Estimating groundwater recharge*, Cambridge University Press.

Hickson, O 2017, 'Surface water and alluvial groundwater connectivity at Mulloon creek and the implications for natural sequence farming', BSc Hons thesis, University of Wollongong, <<https://ro.uow.edu.au/thsci/144>>.

Hiscock, KM 2014, *Hydrogeology: Principles and practice*, John Wiley & Sons.

Isbell, R 2016, *The Australian soil classification*, 2nd edn, CSIRO Publishing, Clayton South, Victoria.

Jenkins, B, Nicholson, A, Moore, L, Harvey, K, Cook, W, Wooldridge, A, Shoemark, V, Nowakowski, A, Muller, R & Winkler, M 2010a, *Hydrogeological landscapes for the Southern Rivers Catchment Management Authority, Braidwood 1:100 000 map sheet: Description document 3 – Moura Creek hydrogeological landscape*, NSW Department of Environment, Climate Change and Water.

Jenkins, B, Nicholson, A, Moore, L, Harvey, K, Cook, W, Wooldridge, A, Shoemark, V, Nowakowski, A, Muller, R & Winkler, M 2010b, *Hydrogeological landscapes for the Southern Rivers Catchment Management Authority, Braidwood 1:100 000 map sheet: Description document 11 – Mulloon hydrogeological landscape*, NSW Department of Environment, Climate Change and Water.

Jenkins, B, Nicholson, A, Moore, L, Harvey, K, Cook, W, Wooldridge, A, Shoemark, V, Nowakowski, A, Muller, R & Winkler, M 2010c, *Hydrogeological landscapes for the Southern Rivers Catchment Management Authority, Braidwood 1:100 000 map sheet: Volume 1 – background, methodology and results*, NSW Department of Environment, Climate Change and Water.

Jenkins, B, Nicholson, A, Wooldridge, A, Moore, L, Harvey, K, Nowakowski, A & Cook, W 2010, 'Hydrogeological landscapes – an expert system for salinity management', *19th World Congress of Soil Science*,

Johnston, P & Brierley, G 2006, 'Late quaternary river evolution of floodplain pockets along Mulloon creek, New South Wales, Australia', *The Holocene*, vol. 16, no. 5, pp. 661-674.

Keene, A, Bush, R & Erskine, W 2007, 'Connectivity of stream water and alluvial groundwater around restoration works in an incised sand-bed stream', *Proceedings of the*

*Fifth Australian Stream Management Conference: Australian Rivers: Making a Difference*, Albury, NSW, pp. 21-25.

King, A, Raiber, M, Cendon, D, Cox, M & Hollins, S 2015, 'Identifying flood recharge and inter-aquifer connectivity using multiple isotopes in subtropical Australia', *Hydrology and Earth System Sciences*, vol. 19, no. 5, pp. 2315-2335.

Mactaggart, B, Bauer, J, Goldney, D & Rawson, A 2008, 'Problems in naming and defining the swampy meadow—an Australian perspective', *Journal of Environmental Management*, vol. 87, no. 3, pp. 461-473.

Maltby, E & Acreman, MC 2011, 'Ecosystem services of wetlands: Pathfinder for a new paradigm', *Hydrological Sciences Journal*, vol. 56, no. 8, pp. 1341-1359.

Massy, C 2017, *Call of the reed warbler: A new agriculture – a new earth*, University of Queensland Press, Brisbane.

Moore, CL, Jenkins, BR, Cowood, AL, Nicholson, A, Muller, R, Wooldridge, A, Cook, W, Wilford, JR, Littleboy, M, Winkler, M & Harvey, K 2018, 'Hydrogeological landscapes framework: A biophysical approach to landscape characterisation and salinity hazard assessment', *Soil Research*, vol. 56, no. 1, pp. 1-18.

Mould, S & Fryirs, K 2017, 'The holocene evolution and geomorphology of a chain of ponds, southeast Australia: Establishing a physical template for river management', *Catena*, vol. 149, pp. 349-362.

Nolan, RH, Boer, MM, Resco de Dios, V, Caccamo, G & Bradstock, RA 2016, 'Large-scale, dynamic transformations in fuel moisture drive wildfire activity across southeastern Australia', *Geophysical Research Letters*, vol. 43, no. 9, pp. 4229-4238.

Norris, D & Andrews, P 2010, 'Re-coupling the carbon and water cycles by natural sequence farming', *International Journal of Water*, vol. 5, no. 4, pp. 386-395.

Norris, RH, Liston, P, Davies, N, Coysh, J, Dyer, F, Linke, S, Prosser, I & Young, B 2001, 'Snapshot of the murray-darling basin river condition', vol.

NSW Government Spatial Services 2015, *Braidwood, 2kmx2km 1-metre resolution digital elevation model*, geospatial database, Department of Finance, Services and Innovation, NSW Government, Sydney, <<https://elevation.fsd.org.au/>>.

Ransley, T, Tottenham, R, Baskaran, S & Brodie, R 2007, *Development of method to map potential stream-aquifer connectivity: A case study in the border rivers catchment*, Bureau of Rural Sciences Canberra.

Rassam, DW, Fellows, CS, De Hayr, R, Hunter, H & Bloesch, P 2006, 'The hydrology of riparian buffer zones; two case studies in an ephemeral and a perennial stream', *Journal of Hydrology*, vol. 325, no. 1-4, pp. 308-324.

Rayleigh, L 1896, 'Theoretical considerations respecting the separation of gases by diffusion and similar processes', *The London, Edinburgh, and Dublin Philosophical Magazine and Journal of Science*, vol. 42, no. 259, pp. 493-498.

Reid, M, Cheng, X, Banks, E, Jankowski, J, Jolly, I, Kumar, P, Lovell, D, Mitchell, M, Mudd, G, Richardson, S, Silburn, D & Werner, A 2009, *Catalogue of conceptual models for groundwater-stream interaction in eastern Australia*, eWater Cooperative Research Centre, Canberra.

Rhoads, BL 2020, *River dynamics: Geomorphology to support management*, Cambridge University Press, New York,  
<<http://ebookcentral.proquest.com/lib/rmit/detail.action?docID=6185922>>.

Short, MA 2017, 'Tracing terrestrial salt cycling using chlorine and bromine', thesis, The Australian National University, Canberra.

Somerville, P, White, I, Macdonald, B, Welch, S & Beavis, S 2006, 'Groundwater and stream water interactions in Widden Brook, Upper Hunter Valley, NSW', *CRC LEME Regional Regolith Symposia 2006*, pp. 326-329.

Sophocleous, M 2002, 'Interactions between groundwater and surface water: The state of the science', *Hydrogeology Journal*, vol. 10, no. 1, pp. 52-67.

Streeton, NA, Greene, RSB, Marchiori, K, Tongway, DJ & Carnegie, MD 2013, 'Rehabilitation of an incised ephemeral stream in central New South Wales, Australia: Identification of incision causes, rehabilitation techniques and channel response', *The Rangeland Journal*, vol. 35, no. 1, pp. 71-83.

Thackway, R 2019, *Assessment of vegetation condition - Mulloon creek catchment and Mulloon community landscape rehydration project, 2018 baseline assessment*, VAST Transformations, for The Mulloon Institute, Canberra.

Tooth, S & Nanson, GC 1995, 'The geomorphology of australia's fluvial systems: Retrospect, perspect and prospect', *Progress in Physical Geography: Earth and Environment*, vol. 19, no. 1, pp. 35-60.

Toscano, G, Acharjee, P, McCormick, C & Devarajan, V 'Water surface elevation calculation using lidar data',

Weber, N & Field, J 'The influence of natural sequence farming stream rehabilitation on upper catchment floodplain soil properties, hunter valley, NSW, Australia', *19th World Congress of Soil Science*,

Williams, J 2010, 'The principles of natural sequence farming', *International Journal of Water*, vol. 5, no. 4, pp. 396-400.

Williams, RT, Fryirs, KA & Hose, GC 2020, 'The hydrological function of a large chain-of-ponds: A wetland system with intermittent surface flows', *Aquatic Sciences*, vol. 82, no. 3, p. 61.

## Appendix 1: Physical parameters (field measurements)

Location	Sample ID	Date	Time	pH	Electrical Conductivity	Temperature (°C)	Electrical Conductivity at 25°C	Redox (mV)	Dissolved Oxygen (mg/L)	Dissolved Oxygen (% sat)	Total Dissolved Solids (mg/L)
T3	MCLRP38	14-Sep-2020	09:20	6.88	149.6	14.5	144.6	314.7	8.89	93.6	90.76
T3	MCLRP39	14-Sep-2020	09:15	7.37	948	16.3	782.4	119.7	3.44	38.3	750.5
T3	MCLRP40	14-Sep-2020	13:00	6.58	402	16.5	346.6	276.6	6.65	73	293.4
T3	MCLRP41-1	14-Sep-2020	14:20	6.31	214.7	15.3	199.3	337.6	6.12	64.9	131.1
T3	MCLRP42-1	14-Sep-2020	15:10	5.92	290.7	16.1	244.7	234.9	1.31	14.5	160.5
T3	MCLRP43	14-Sep-2020	15:50	6.04	523	14.8	414.0	155.7	1.42	15.1	279.9
T3	MCLRP44	14-Sep-2020	16:20	6.02	478	14.6	481.7	157	2.6	27.9	352.5
T3	MCLRP45	15-Sep-2020	08:00	6.36	233.6	13.7	200.5	349.4	8.12	84	132.7
T3	MCLRP46	15-Sep-2020	09:20	7.25	780	16.6	682.5	181	7.85	85.8	580.2
T3	MCLRP47	15-Sep-2020	09:35	6.32	695	12.9	609.7	269.3	9.06	91.2	351.7
T3	MCLRP48	15-Sep-2020	10:15	6.71	5980	15.1	4984.3	281.6	4.91	53.2	3458
T4	MCLRP50	15-Sep-2020	13:15	7.25	1676	15.9	1339.1	260.1	10.11	109.3	1062
T4	MCLRP51	18-Sep-2020	22:00	6.61	169.2	11.7	140.8	281.6	6.74	66.4	104.8
T4	MCLRP52	18-Sep-2020	11:00	6.68	182.9	12	151.1	356.9	8.68	84.9	105.3
T4	MCLRP53	18-Sep-2020	09:55	7.83	1249	11.9	1107.5	204.6	6.27	62.3	820.3
T4	MCLRP54	18-Sep-2020	09:55	7.62	1265	12.3	1082.6	208.9	6.81	68	849.1
T4	MCLRP55	17-Sep-2020	11:00	7.04	553	12.8	417.3	216.2	9.46	96.1	308.8
T4	MCLRP56	17-Sep-2020	11:00	6.66	262.4	14	207.7	146.4	6.45	68.5	164.1
T4	MCLRP57	17-Sep-2020	09:30	6.56	192.6	12.6	178.0	295	19.06	195.2	128
T4	MCLRP58	17-Sep-2020	09:30	7.02	223.7	12.6	195.2	281.1	8.25	83.9	120.2
T4	MCLRP59	17-Sep-2020	08:50	7.62	3160	14.3	2594.3	203.1	6.43	65.4	2062
T4	MCLRP60	17-Sep-2020	08:45	7.58	2954	14.7	2455.9	76.3	2.37	24.1	2079
T4	MCLRP77	18-Sep-2020	12:00	7.54	544	14.6	442.4	57	0.11	1	395.5
Stream	Palerang Crossing	15-Sep-2020	11:55	7.18	116.2	16.7	110.2	268.3	13.23	143.7	79.89
Stream	T3 Leaky Weir	15-Sep-2020	09:00	6.7	120.1	14	110.8	354	15.65	159.1	78.39
Stream	T3 Leaky Weir	17-Sep-2020	10:40	6.88	122.4	15.2	116.7	265	14.27	151.4	79.44
Stream	T4 Laneway North	17-Sep-2020	12:00	7.32	123.5	15.7	112.7	244.6	10.97	118.9	78.94

## Appendix 2: Major ions

Location	Sample ID	Major Cations (mg/kg)				Anions (mg/kg)							
		Ca	Mg	Na	K	Cl	SO <sub>4</sub>	Total Alkalinity as HCO <sub>3</sub>	Br	F	NO <sub>2</sub>	NO <sub>3</sub>	PO <sub>4</sub>
T3	MCLRP38	2.39	2.13	30.76	0.96	16.90	11.20	18.53	0.10	0.10	<1	7.79	<0.1
T3	MCLRP39	46.98	37.53	107.49	3.19	91.38	17.34	443.08	0.28	1.39	<1	2.10	<0.1
T3	MCLRP40	12.67	10.52	59.86	1.3	37.50	14.48	145.86	0.15	0.45	<1	10.79	<0.1
T3	MCLRP41-1	8.97	9.29	15.79	0.91	20.46	15.77	43.21	0.07	0.13	<1	16.56	<0.1
T3	MCLRP42-1	14.39	7.48	29.04	2.58	43.96	0.03	62.06	0.09	0.10	<1	0.87	<0.1
T3	MCLRP43	20.1	10.7	39.4	2.28	80.17	22.34	104.48	0.11	0.11	<1	0.32	<0.1
T3	MCLRP44	33.7	13	45.5	4.7	63.28	23.17	168.90	0.17	0.11	<1	0.11	<0.1
T3	MCLRP45	9.8	6.73	20.08	0.46	35.43	9.40	43.99	0.08	0.22	<1	6.54	<0.1
T3	MCLRP46	26.22	6.85	150.9	1.79	111.54	8.35	271.03	0.33	2.80	<1	0.71	<0.1
T3	MCLRP47	20.31	10.4	87.79	0.1	178.31	12.31	40.65	0.30	0.56	<1	1.30	<0.1
T3	MCLRP48	141.11	271.28	616.04	3.31	2073.00	89.90	182.33	<0.05	19.00		62.00	
T4	MCLRP50	53.27	95.09	138.52	2.35	284.48	40.93	440.28	1.24	0.42	<1	6.48	<0.1
T4	MCLRP51	5.23	7.03	14.4	0.65	17.37	6.53	48.71	0.10	0.10	<1	4.78	<0.1
T4	MCLRP52	4.93	7.46	12.84	3.43	20.03	4.48	37.66	0.10	0.21	<1	14.28	<0.1
T4	MCLRP53	54.48	51.47	147.72	3.15	178.81	122.23	258.25	0.47	0.90	<1	3.26	<0.1
T4	MCLRP54	56.26	51.92	110.63	0.83	187.23	124.11	315.03	0.52	0.63	<1	2.42	<0.1
T4	MCLRP55	22.04	15.36	67.69	1.18	66.37	0.07	134.21	0.13	0.46	<1	1.41	<0.1
T4	MCLRP56	13.43	7.48	25.42	0.72	25.48	0.05	91.13	0.09	0.23	<1	0.18	<0.1
T4	MCLRP57	4.26	1.62	29.49	0.84	14.08	36.43	39.16	<0.05	0.11	<1	1.97	<0.1
T4	MCLRP58	7.96	5.07	20.43	0.45	41.14	11.70	30.64	0.09	0.08	<1	2.76	<0.1
T4	MCLRP59	69.37	41.79	514.21	3.02	395.87	701.94	308.76	1.16	1.11	<1	25.88	<0.1
T4	MCLRP60	59.3	35	496.47	9.29	316.96	696.37	463.50	1.05	1.45	<1	0.45	0.6
T4	MCLRP77	7.36	5.66	98.88	0.89	63.74	9.10	207.40	0.17	2.05	<1	0.47	<0.1
Stream	Palerang Crossing	5.85	3.12	9.75	1.62	14.50	9.51	35.35	<0.05	0.05	<1	0.13	<0.1
Stream	T3 Leaky Weir	5.81	3.16	9.99	1.1	15.33	9.75	33.00	<0.05	0.05	<1	0.20	<0.1
Stream	T3 Leaky Weir	6.89	3.83	9.99	1.39	16.20	9.51	31.42	<0.05	0.06	<1	0.15	<0.1
Stream	T4 Laneway North	6.08	3.29	9.64	1.68	16.16	9.59	32.21	<0.05	0.06	<1	0.23	<0.1

## Appendix 3: Hydraulic gradient calculations

	Location A	Location B	Head loss (m)	Horizontal distance between points (m)	Gradient*
<b>Transect 3</b>	38	39	15.10	0	N/A
	39	40	0.18	84	0.000
	40	41	-0.66	133	-0.005
	41	42	1.70	90	0.019
	42	43	-0.01	7	0.000
	43	44	0.21	13	0.000
	44	stream	0.91	20	0.045
	stream	45	0.90	231	0.004
	45	46	-0.12	116	0.000
	46	47	-0.15	0	0.000
	46	48	-0.88	199	-0.004
	38	stream	17.43	347	0.050
	39	stream	2.33	347	0.007
	stream	48	-1.89	395	-0.005
<b>Transect 4</b>	50	51	-1.80	86	-0.021
	51	53	0.39	115	0.003
	53	77	-0.42	101	-0.004
	77	55	0.19	118	0.000
	55	stream	1.18	31	0.038
	stream	57	-0.90	91.6	-0.010
	57	59	1.79	263.4	0.007
	stream	59	0.90	355	0.003

\* DEM data have 0.3 m vertical accuracy, so head differences <0.3 m are recorded as 0 m



## Appendix 4: Trace elements

Location	Sample ID	Aluminium	Arsenic	Barium	Beryllium	Cadmium	Chromium	Cobalt	Copper	Iron	Lead
T3	MCLRP38	0.207	0.001	0.153	0.000	0.000	0.005	0.001	0.039	0.037	0.001
T3	MCLRP39	0.071	0.009	0.221	0.000	0.000	0.000	0.000	0.137	0.812	0.433
T3	MCLRP40	0.046	0.000	0.067	0.000	0.000	0.000	0.000	0.003	0.033	0.018
T3	MCLRP41-1	6.631	0.002	0.107	0.000	0.000	0.011	0.003	0.036	5.307	0.119
T3	MCLRP42-1	0.052	0.002	0.086	0.000	0.000	0.001	0.001	0.005	4.269	0.030
T3	MCLRP43	0.024	0.004	0.093	0.000	<0.000012	0.001	0.003	0.005	14.146	0.018
T3	MCLRP44	0.030	0.004	0.113	0.000	0.000	0.001	0.005	0.001	27.740	0.009
T3	MCLRP45	0.023	0.000	0.044	0.000	0.000	0.000	0.000	0.002	0.282	0.006
T3	MCLRP46	0.049	0.003	0.061	0.000	0.000	0.000	0.001	0.004	0.473	0.004
T3	MCLRP47	0.084	0.000	0.093	0.000	0.000	0.000	0.000	0.005	0.027	0.001
T3	MCLRP48	<0.000968	0.000	0.190	0.000	0.002	0.000	0.019	<0.000161	<0.000121	<0.000024
T4	MCLRP50	0.002	0.001	0.323	0.000	0.000	0.001	0.000	<0.000161	<0.000121	<0.000024
T4	MCLRP51	0.023	0.000	0.038	0.000	0.000	0.000	0.000	0.005	0.127	0.011
T4	MCLRP52	0.347	0.001	0.062	0.000	<0.000012	0.000	0.002	0.001	0.090	0.000
T4	MCLRP53	0.004	0.000	0.248	0.000	<0.000012	0.001	0.000	<0.000161	<0.000121	<0.000024
T4	MCLRP54	0.017	0.000	0.150	0.000	0.000	0.000	0.000	0.002	0.020	0.010
T4	MCLRP55	0.028	0.000	0.043	0.000	0.000	0.000	0.000	0.001	0.001	0.001
T4	MCLRP56	0.068	0.005	0.052	0.000	<0.000012	0.001	0.002	0.004	3.538	0.005
T4	MCLRP57	0.185	0.000	0.054	0.000	<0.000012	0.000	0.002	0.001	0.041	0.000
T4	MCLRP58	0.012	0.000	0.031	0.000	<0.000012	0.000	0.000	0.001	0.055	0.002
T4	MCLRP59	0.005	0.001	0.077	0.000	0.000	0.001	0.002	0.011	0.005	<0.000024
T4	MCLRP60	0.019	0.002	0.174	0.000	0.000	0.000	0.003	0.001	2.634	0.003
T4	MCLRP77	0.014	0.001	0.022	0.000	<0.000012	0.000	0.000	0.002	0.480	0.001
Stream	Palerang Crossing	0.030	0.001	0.029	0.000	0.000	0.000	0.000	0.003	0.122	0.001
Stream	T3 Leaky Weir	0.028	0.001	0.029	0.000	0.000	0.000	0.000	0.003	0.098	0.002
Stream	T3 Leaky Weir	0.033	0.001	0.035	0.000	<0.000012	0.000	0.000	0.001	0.220	0.000
Stream	T4 Laneway North	0.034	0.001	0.030	0.000	0.000	0.000	0.000	0.004	0.228	0.001

Location	Sample ID	Manganese	Molybdenum	Nickel	Selenium	Silver	Thallium	Thorium	Uranium	Vanadium	Zinc
T3	MCLRP38	0.006	0.000	0.007	<0.000589	<0.000013	0.000	<0.000025	0.000	0.001	0.218
T3	MCLRP39	0.067	0.002	0.001	<0.000589	0.000	<0.000008	<0.000025	0.002	0.000	0.085
T3	MCLRP40	0.037	0.001	0.001	0.001	<0.000013	<0.000008	<0.000025	0.000	0.000	0.016
T3	MCLRP41-1	0.193	0.000	0.006	0.003	0.000	0.000	0.002	0.001	0.014	0.034
T3	MCLRP42-1	0.312	0.000	0.002	<0.000589	0.000	<0.000008	<0.000025	0.000	0.001	0.022
T3	MCLRP43	0.773	0.000	0.003	<0.000589	0.000	<0.000008	<0.000025	0.000	0.005	0.018
T3	MCLRP44	1.524	0.000	0.002	<0.000589	0.000	<0.000008	<0.000025	0.000	0.001	0.009
T3	MCLRP45	0.014	0.000	0.001	<0.000589	0.000	<0.000008	<0.000025	<0.000004	0.000	0.014
T3	MCLRP46	0.071	0.003	0.001	<0.000589	0.000	<0.000008	<0.000025	0.002	0.000	0.039
T3	MCLRP47	0.008	0.000	0.001	<0.000589	<0.000013	<0.000008	<0.000025	<0.000004	0.013	0.005
T3	MCLRP48	2.983	0.001	0.017	<0.000589	0.000	0.000	<0.000025	0.000	0.012	0.004
T4	MCLRP50	0.058	0.001	0.001	0.001	<0.000013	0.000	<0.000025	0.009	0.001	<0.000144
T4	MCLRP51	0.012	0.000	0.002	<0.000589	<0.000013	<0.000008	<0.000025	0.000	0.000	0.015
T4	MCLRP52	0.103	0.000	0.001	<0.000589	0.000	<0.000008	<0.000025	<0.000004	0.000	0.008
T4	MCLRP53	0.005	0.001	0.000	0.002	<0.000013	<0.000008	<0.000025	0.011	0.001	<0.000144
T4	MCLRP54	0.011	0.001	0.001	0.002	0.000	<0.000008	<0.000025	0.008	0.000	0.011
T4	MCLRP55	0.003	0.000	0.000	<0.000589	<0.000013	<0.000008	<0.000025	0.000	0.001	0.011
T4	MCLRP56	0.490	0.001	0.001	<0.000589	0.000	<0.000008	<0.000025	0.000	0.003	0.009
T4	MCLRP57	0.099	0.000	0.003	<0.000589	0.000	<0.000008	<0.000025	0.000	0.000	0.030
T4	MCLRP58	0.006	0.000	0.001	<0.000589	<0.000013	<0.000008	<0.000025	0.000	0.000	0.011
T4	MCLRP59	0.840	0.055	0.006	0.006	0.000	0.000	<0.000025	0.054	0.003	0.010
T4	MCLRP60	2.514	0.040	0.002	0.001	0.000	<0.000008	<0.000025	0.015	0.000	0.032
T4	MCLRP77	0.116	0.001	0.000	<0.000589	0.000	<0.000008	<0.000025	0.001	0.000	0.006
Stream	Palerang Crossing	0.051	0.000	0.002	<0.000589	0.001	<0.000008	<0.000025	0.000	0.000	0.011
Stream	T3 Leaky Weir	0.055	0.000	0.002	<0.000589	0.001	<0.000008	<0.000025	0.000	0.000	0.005
Stream	T3 Leaky Weir	0.125	<0.000038	0.001	<0.000589	0.000	<0.000008	<0.000025	<0.000004	0.000	0.004
Stream	T4 Laneway North	0.094	0.000	0.001	<0.000589	0.001	<0.000008	<0.000025	0.000	0.000	0.009

## Appendix 5: Stable water isotopes

Location	Sample ID	$\delta^{18}\text{O}$ (‰ VSMOW)	$\delta^{18}\text{O}$ Standard Deviation	$\delta^2\text{H}$ (‰ VSMOW)	$\delta^2\text{H}$ Standard Deviation	Deuterium excess
T3	MCLRP38	-8.90	0.06	-53.90	0.26	17.28
T3	MCLRP39	-7.81	0.06	-45.96	0.15	16.49
T3	MCLRP40	-7.73	0.03	-44.53	0.14	17.27
T3	MCLRP41-1	-7.61	0.04	-45.19	0.21	15.67
T3	MCLRP42-1	-5.31	0.02	-30.87	0.11	11.60
T3	MCLRP43	-6.24	0.02	-37.96	0.27	11.86
T3	MCLRP44	-6.34	0.32	-37.14	0.71	13.58
T3	MCLRP45	-5.54	0.02	-32.43	0.27	11.84
T3	MCLRP46	-7.71	0.01	-45.87	0.10	15.87
T3	MCLRP47	-7.34	0.12	-44.78	0.37	13.97
T3	MCLRP48			not measured		
T4	MCLRP50	-8.05	0.14	-48.26	0.15	16.21
T4	MCLRP51	-8.63	0.10	-52.84	0.28	16.26
T4	MCLRP52	-8.50	0.03	-51.08	0.11	16.90
T4	MCLRP53	-8.05	0.12	-48.18	0.76	16.24
T4	MCLRP54	-7.91	0.05	-46.58	0.17	16.78
T4	MCLRP55	-5.56	0.05	-32.41	0.21	12.17
T4	MCLRP56	-6.60	0.01	-37.13	0.12	15.61
T4	MCLRP57	-8.68	0.07	-55.19	0.36	14.22
T4	MCLRP58	-5.97	0.03	-36.08	0.14	11.72
T4	MCLRP59	-6.94	0.02	-42.71	0.25	12.78
T4	MCLRP60	-6.15	0.05	-37.32	0.08	11.88
T4	MCLRP77	-8.37	0.02	-50.08	0.06	16.91
Stream	Palerang Crossing	-7.36	0.05	-41.48	0.29	17.36
Stream	T3 Leaky Weir	-7.23	0.15	-41.17	0.63	16.85
Stream	T3 Leaky Weir	-7.16	0.04	-40.99	0.09	16.32
Stream	T4 Laneway North	-6.93	0.05	-39.83	0.09	15.56